Magazine of Civil Engineering. 2019. 92(8). Pp. 3–26
Инженерно-строительный журнал. 2019. № 8(92). С. 3–26

Magazine of Civil Engineering

ISSN 2071-0305

journal homepage: http://engstroy.spbstu.ru/

DOI: 10.18720/MCE.92.1

Algorithm for shear flows in arbitrary cross-sections of thin-walled bars

V. Yurchenko*
Kyiv National University of Construction and Architecture, Kyiv, Ukraine
** E–mail: vitalinay@rambler.ru*

Keywords: thin-walled bar, arbitrary cross-section, shear forces flow, closed contour, graph theory, numerical algorithm, numerical examples, software implementation

Abstract. Development of a general computer program for the design and verification of thin-walled bar structural members remains an actual task. Despite the prevailing influence of normal stresses on the stress-strain state of thin-walled bars design and verification of thin-walled structural members should be performed taking into account not only normal stresses, but also shear stresses. Therefore, in the paper a thin-walled bar of an arbitrary cross-section which is undergone to the general load case is considered as investigated object. The main research question is development of mathematical support and knoware for numerical solution for the shear stresses problem with orientation on software implementation in a computer-aided design system for thin-walled bar structures. The problem of shear stresses outside longitudinal edges of an arbitrary cross-section (including open-closed multi-contour cross-sections) of a thin-walled bar subjected to the general load case has been considered in the paper. The formulated problem has been reduced to the searching problem for unknown shear forces flows that have the least value of the Castigliano's functional. Besides, constraints-equalities of shear forces flows equilibrium formulated for cross-section branch points, as well as equilibrium equation formulated for the whole cross-section relating to longitudinal axes of the thin-walled bar have been taken into account. A detailed numerical algorithm intended to solve the formulated problem has been proposed by the paper. The algorithm is oriented on software implementation in systems of computer-aided design of thin-walled bar structures. Developed algorithm has been implemented in SCAD Office environment by the program TONUS. Numerical examples for calculation of thin-walled bars with open and open-closed multi-contour cross-sections have been considered in order to validate developed algorithm and verify calculation accuracy for sectorial cross-section geometrical properties and shear stresses caused by warping torque and shear forces. Validity of the calculation results obtained using developed software has been proven by considered examples.

1. Introduction

To provide desired stiffness and strength in torsion, bridge superstructures are often constructed with a cross-section consisting of multiple cells (Figure 1) which have thin walls relative to their overall dimensions. When the cross-section contains multiple cells, they all provide resistance to applied torsion and for elastic continuity each cell must twist the same amount. With these considerations, equilibrium and compatibility conditions allow simultaneous equations to be formed and solved to determine the shear flow for each cell [1].

The behavior of single-box multi-cell box-girders with corrugated steel webs under pure torsion has been considered by Kongjian Shen et al. [2]. Experimental and numerical studies for considered structures have been also performed [3].

Dowell and Johnson proposed a relaxation method that distributes incremental shear flows back and forth between cells, reducing errors with each distribution cycle, until the final shear flows for all cells approximate the correct values. A closed-form approach has been introduced to determine, exactly, both the torsional constant and all shear flows for multi-cell cross-sections under torsion in the paper [1].

The problem of shear stresses determination for thin-walled bars has been also studied by Slivker in [4, 5] for the general loading case. His semi-sheared theory has been applied by Lalin et al. [6, 7] and Dyakov [8]

Yurchenko, V. Algorithm for shear flows in arbitrary cross-sections of thin-walled bars. Magazine of Civil Engineering. 2019. 92(8). Pp. 3–26. DOI: 10.18720/MCE.92.1

Юрченко В. Алгоритм определения потоков касательных усилий для произвольных сечений тонкостенных стержней // Инженерно-строительный журнал. 2019. № 8(92). С. 3–26. DOI: 10.18720/MCE.92.1

for the stability problems of thin-walled bars.

Further investigations in this area require the development of a detailed algorithm intended to software implementation in a computer-aided design system for thin-walled structures [9]. Such algorithm can be validated against benchmark examples as well as finite element results [10, 11]. It is reasonable to construct this algorithm using the mathematical apparatus of the graph theory as it is convenient to describe the topological properties of multi-cellular cross-section [12].

The graph algorithm used in this paper is given first by Tarjan [13]. Its application in analysis of thin-walled multi-cellular section is described by Alfano et al. [14], but the distribution of torsion stresses due to a change in normal stresses has not been considered. The graph theory has been also applied in [15, 16] to calculate the geometrical cross-sectional properties of thin-walled bars with hybrid (open-closed) types of cross-sections.

A simple computer program has been developed by Chai H. Yoo et al. [17] to evaluate the bending shear flow of any multiply-connected cellular sections. Prokić has developed a computer program for the determination of the torsional and flexural properties of thin-walled beams with arbitrary open-closed cross-section. In his paper [18] graph theory has been also applied to establish the topological properties of multi-cellular cross-section. Gurujee and Shah [19] presented a general purpose computer program capable of analyzing any planar frame made up of thin-walled structural members. Choudhary and Doshi proposed an algorithm for shear stress evaluation in ship hull girders [20].

Although many papers are published on the behavior of thin-walled bars, the development of a general computer program for the design and verification of thin-walled structural members remains an actual task. Despite the prevailing influence of normal stresses on the stress-strain state of thin-walled bars, the design and verification of thin-walled structural members should be performed taking into account not only normal stresses, but also shear stresses. Therefore, in this paper, a thin-walled bar of an arbitrary cross-section under the general load case is considered as *investigated object*. The main *research question* is the development of mathematical support and software for numerical solution for the shear stresses problem with orientation on software implementation in a computer-aided design system for the thin-walled structures.

2. Methods

2.1. Problem formulation

Let us consider the problem of shear stresses on longitudinal edges of an arbitrary section of a thin-walled bar that consists of several closed (connected and/or disconnected) contours and/or also open parts. Let us introduce in the plane of thin-walled cross-section a Cartesian coordinate system y_cOz_c with the origin in the center of mass C of the section, the direction of the coordinate system axes y_cOz_c coincides with the direction of principle axes of inertia. Let us also introduce in the plane of thin-walled cross-section a Cartesian coordinate system y_sOz_s with the origin in the shear center S of the section, the direction of the coordinate system axes y_sOz_s coincides with the direction of principle axes of inertia.

Let us introduce in further consideration the system of angular position coordinate with the origin in a certain (generally randomly selected) sectional point. Each considered sectional point can be associated with the angular position ς. The value ς should be calculated as the geometrical length of the curve constructed from the origin to the considered sectional point taken along the sectional contour. We also assume that the increment of the angular position ς corresponds to the positive direction of section path tracing.

We assume that the integral geometrical properties of the section are known: A is the cross-sectional area, I_y and I_z are the second moments of area relative to the main axes of inertia which coincide with axes of global Cartesian coordinate system y_cOz_c; I_ω is the sectorial moment of inertia; I_t is the second moment of area for pure torsion. We also assume that Young's modulus E and shear modulus G are constant for the whole cross-section of the thin-walled bar.

Generally, the thin-walled bar is subjected to the action of eight force factors. Axial force N, bending moments M_y and M_z relative to the principle axes of inertia and warping bimoment B are applied at the center of mass C (see Figure 2) of the section and cause normal stresses in the cross-section $\sigma_i(x, \varsigma)$:

$$\sigma_i\left(x,\varsigma\right)=\frac{N\left(x\right)}{A}+\frac{M_y\left(x\right)}{I_y}z_i\left(\varsigma\right)+\frac{M_z\left(x\right)}{I_z}y_i\left(\varsigma\right)+\frac{B\left(x\right)}{I_\varpi}\varpi_i\left(\varsigma\right), \tag{1.1}$$

where $y_i\left(\varsigma\right), z_i\left(\varsigma\right), \varpi_i\left(\varsigma\right)$ are the coordinates and sectorial coordinate of the considered point in cross-section of a thin-walled bar.

Figure 1. Box-girder bridge multi-cell cross-section [23].

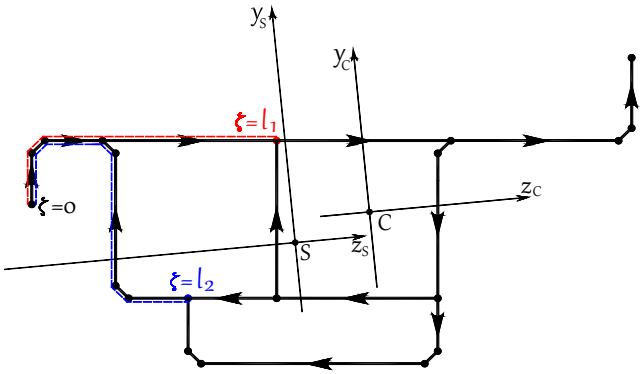

Figure 2. Cross-section of a thin-walled bar with representation of different angular positions as examples.

Shear forces Q_y and Q_z, total torque M_x and warping torque M_ω are applied at the shear center S (see Figure 2) of the cross-section and cause shear stresses in the cross-section, which can be written in terms of shear forces flows $T_j(x, \varsigma)$ as presented below:

$$\tau_j(x,\varsigma) = \frac{T_j(x,\varsigma)}{\delta_j(\varsigma)}, \tag{1.2}$$

where $\delta_j(\varsigma)$ is the thickness of j^{th} section element.

An arbitrary section of the thin-walled bar can be described by the set of sectional points $\mathbf{P} = \left\{ \vec{p}_p = \left\{ y_p, z_p \right\} \mid p = \overline{1, n_p} \right\}$ (y_p and z_p are the coordinates of p^{th} sectional point in the global Cartesian coordinate system yOz) and by the set of sectional segments $\mathbf{S} = \left\{ \vec{s}_s = \left\{ p_s^{st}, p_s^{end} \right\} \mid s = \overline{1, n_s} \right\}$, which connect some two adjacent sectional points (Figure 3), where n_p and n_s are the numbers of the sectional points and segments, respectively.

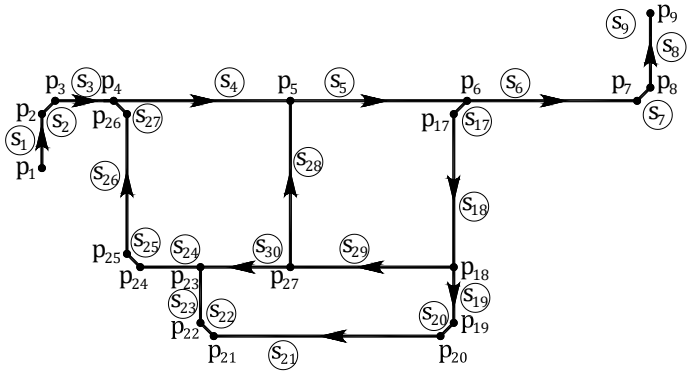

Figure 3. Arbitrary cross-section of a thin-walled bar determined on the set of sectional points $\mathbf{P}$ and set of sectional segments $\mathbf{S}$.

The specified segment thickness $\boldsymbol{\delta} = \left\{ \delta_s \mid s = \overline{1, n_s} \right\}$ corresponds to each sectional segment. The set of sectorial coordinates $\boldsymbol{\omega} = \left\{ \omega_p \mid p = \overline{1, n_p} \right\}$ and the set of normalized sectorial coordinates $\varpi = \left\{ \varpi_p \mid p = \overline{1, n_p} \right\}$ of the section correspond to the set of the sectional points $\mathbf{P}$, assuming that the values of the sectorial coordinates and normalized sectorial coordinates in each cross-sectional point are known.

The set of angular positions $\boldsymbol{\varsigma} = \left\{ \vec{\varsigma}_\kappa = \left\{ \varsigma_\kappa^{start}, \varsigma_\kappa^{end} \right\} \mid \kappa = \overline{1, n_\varsigma - 1} \right\}$ is actually intended to implement a numerical integration taken along the thin-walled section contour (e.g., when calculating geometrical properties of the cross-section, values of shear forces flows, etc.), where κ is the number of a segment, $n_\varsigma - 1$ is the number of the sectional segments. It should be noted that the angular positions are attributes of the ends of the sectional segments.

The initial data about the thin-walled section should be mapped onto the set of the angular positions ς, $\kappa = \overline{1, n_\varsigma - 1}$ by means of corresponding sets of sectional segments $\mathbf{S}^\varsigma = \{\vec{s}_\kappa^{\,\varsigma} = \{\varsigma_\kappa^{start}, \varsigma_\kappa^{end}\} : \varsigma_\kappa^{start}, \varsigma_\kappa^{end} \subseteq \boldsymbol{\varsigma}\}$, set of sectorial coordinates $\boldsymbol{\omega}^\varsigma = \left\{\vec{\omega}_\kappa^{\,\varsigma} = \left\{\omega_\kappa^{start}, \omega_\kappa^{end}\right\} : \omega_\kappa^{start}, \omega_\kappa^{end} \subseteq \boldsymbol{\omega}\right\}$ for the ends of sectional segments as well as the set of thicknesses $\boldsymbol{\delta}^\varsigma = \left\{\delta_\kappa^\varsigma \subseteq \boldsymbol{\delta}\right\}$ for the segments, $\kappa = \overline{1, n_\varsigma - 1}$.

2.2. Distribution of shear forces flows along closed contours of an arbitrary cross-section of thin-walled bar

2.2.1. Construction of connected graph G^ς associated with a section of a thin-walled bar

An arbitrary cross-section of a thin-walled bar can be associated with a planar connected non-oriented graph $\mathbf{G}^\varsigma$ determined on the sets of $\mathbf{G}^\varsigma = \{\mathbf{V}, \mathbf{R}\}$, where $\mathbf{V}$ is the finite set of the graph vertices, $\mathbf{R}$ is the set of the graph edges or the set of unordered pairs on $\mathbf{V}$ (Figure 4) [21, 22]. Herewith, for each graph edge $\mathbf{r} = \{u, v\} \in \mathbf{R}$ we assume that $u \neq v$.

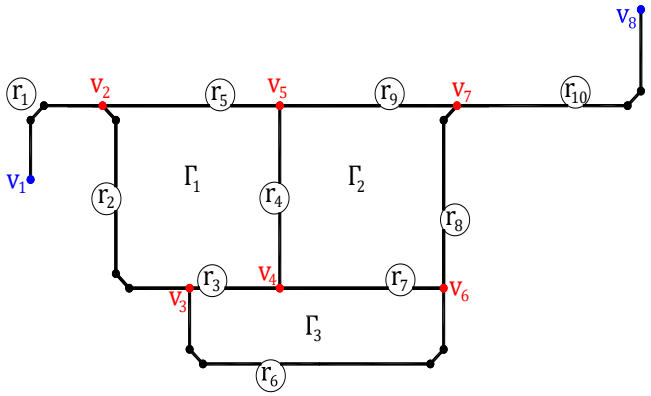

Figure 4. Graph $\mathbf{G}^\varsigma$ associated with cross-section of thin-walled bar (the branch points are highlighted in red, while the end points are highlighted in blue).

The vertices of the graph $\mathbf{G}^\varsigma$ are associated with *characteristic sectional points* only, which can be either:

1) *branch points*, i.e. sectional points connected with more than two sectional segments, $\mathbf{v}^\mathbf{p} = \left\{\vec{p}_v \mid v = \overline{1, n_v}\right\}$, here n_v is the number of these points;

2) *end points*, i.e. sectional points connected with only one sectional segment $\mathbf{v}_{end}^\mathbf{p} = \left\{\vec{p}_g \mid g = \overline{1, n_g}\right\}$, here n_g is the number of these points.

The edges of the graph $\mathbf{G}^\varsigma$ are associated with sectional parts located between characteristic sectional points (with *unbranched sectional parts*). An edge of the graph $\mathbf{G}^\varsigma$, as a rule, may contain several sectional segments, so the full information about edge $\mathbf{R}_j^\varsigma$ of the graph can be described by the set of sectional segments $\vec{s}_r^{\,\varsigma}$, $r = \overline{1, n_{\varsigma rj}}$, from the array $\mathbf{S}^\varsigma = \left\{\vec{s}_\kappa^{\,\varsigma} = \left\{\varsigma_\kappa^{start}, \varsigma_\kappa^{end}\right\} \mid \kappa = \overline{1, n_\varsigma - 1}\right\}$, $\vec{s}_r^{\,\varsigma} \in \mathbf{S}^\varsigma$, belonging to considered graph edge, $\vec{s}_r^{\,\varsigma} \in \mathbf{R}_j$: $\mathbf{R}_j^\varsigma = \left\{\vec{s}_r^{\,\varsigma} : \vec{s}_r^{\,\varsigma} \in \mathbf{S}^\varsigma \wedge \vec{s}_r^{\,\varsigma} \in \mathbf{R}_j \mid r = \overline{1, n_{\varsigma rj}}\right\}$, here $n_{\varsigma rj}$ is the number of segments for j^{th} graph edge. The set of all the graph edges defined on the set of segments $\mathbf{S}^\varsigma$ can be expressed as $\mathbf{R}^\varsigma = \left\{\mathbf{R}_j^\varsigma \mid j = \overline{1, n_r}\right\}$.

We also assume that the arbitrary section of the thin-walled bar may contain some quantity of closed contours. Each closed contour is associated with a cycle of the graph $\mathbf{G}^\varsigma$ or with a vertices sequence $v_0^k, v_1^k, v_2^k, ..., v_n^k$, such that $v_i^k \mapsto v_{i+1}^k \forall i \Leftrightarrow \exists v_{i+1}^k$, where n_k is the number of closed contours in the section (the number of the graph $\mathbf{G}^\varsigma$ cycles).

Some closed contour of a section $\mathbf{\Gamma}_k^{r\varsigma}$ (a basic cycle of the graph $\mathbf{G}^{\varsigma}$) can be definitely determined by the set of the graph edges $\mathbf{R}_j^{\varsigma} \in \mathbf{R}^{\varsigma}$ belonging to the considered contour $\mathbf{\Gamma}_k^{r\varsigma} = \left\{ \mathbf{R}_j^{\varsigma} \mid j = \overline{1, n_{r\varsigma\Gamma_k}} \right\}$, where $n_{r\varsigma\Gamma_k}$ is the number of the graph edges belonging to k^{th} closed contour. Besides, it is convenient to have the mapping of the closed contour $\mathbf{\Gamma}_k^{r\varsigma}$ onto the set of sectional segments $\vec{s}_m^{\varsigma}$, $\vec{s}_m^{\varsigma} \in \mathbf{S}^{\varsigma}$, belonging to the considered closed contour, $\forall m = \overline{1, n_{\varsigma\Gamma_k}}$: $\mathbf{\Gamma}_k^{\varsigma} = \left\{ \vec{s}_m^{\varsigma} : \vec{s}_m^{\varsigma} \in \mathbf{S}^{\varsigma}, \exists \mathbf{R}_{\alpha}^{\varsigma} \subseteq \mathbf{R}^{\varsigma} : \vec{s}_m^{\varsigma} \subseteq \mathbf{R}_{\alpha}^{\varsigma} \wedge \mathbf{R}_{\alpha}^{\varsigma} \subseteq \mathbf{\Gamma}_k^{r\varsigma} \right\}$, here $n_{\varsigma\Gamma_k}$ is the number of the sectional segments belonging to k^{th} closed contour.

The closed contours (basic cycles of the graph $\mathbf{G}^{\varsigma}$) defined on the set of graph edges $\mathbf{R}^{\varsigma}$ and on the set of section segments $\mathbf{S}^{\varsigma}$ can be described as $\mathbf{\Phi}^{r\varsigma} = \left\{ \mathbf{\Gamma}_k^{r\varsigma} \mid k = \overline{1, n_k} \right\}$ and $\mathbf{\Phi}^{\varsigma} = \left\{ \mathbf{\Gamma}_k^{\varsigma} \mid k = \overline{1, n_k} \right\}$, respectively. It should be noted that the identification of closed contours in the section $\mathbf{\Phi}^{r\varsigma}$ and $\mathbf{\Phi}^{\varsigma}$ can be easily implemented using depth-first search algorithms on the graph.

Let us compose an incidence matrix $\dot{\mathbf{I}}$ for the graph $\mathbf{G}^{\varsigma}$ with dimensions $n_v \times n_r$, $\dot{\mathbf{I}} = \left\{ g_{ij} \mid i = \overline{1, n_v},\ j = \overline{1, n_r} \right\}$. The components of the matrix take the following values: $g_{ij} = 1$, if i^{th} graph vertex is a start vertex for j^{th} edge; $g_{ij} = -1$, if i^{th} graph vertex is an end vertex for j^{th} edge; $g_{ij} = 0$, otherwise. Let us also introduce a matrix $\left|\dot{\mathbf{I}}\right| = \left\{ \left| g_{ij} \right| \mid i = \overline{1, n_v},\ j = \overline{1, n_r} \right\}$ composed of the modulus of elements g_{ij} of the matrix $\dot{\mathbf{I}}$.

Next, we can compose a matrix of basic graph cycles $\mathbf{F}$ with dimensions $n_k \times n_k$, $\mathbf{F} = \left\{ f_{kj} \right\}$, $k = \overline{1, n_k}$, $j = \overline{1, n_r}$. The components of the matrix take the following values: $f_{kj} = 1$, if j^{th} graph edge belongs to k^{th} basic graph cycle $\left(\mathbf{R}_j^{\varsigma} \subseteq \mathbf{\Gamma}_k^{\varsigma} \right)$ and the edge direction coincides with the positive direction of path tracing; $f_{kj} = -1$, if j^{th} graph edge belongs to k^{th} basic graph cycle $\left(\mathbf{R}_j^{\varsigma} \subseteq \mathbf{\Gamma}_k^{\varsigma} \right)$ and the edge direction does not coincide with the positive direction of path tracing; $f_{kj} = 0$,, if j^{th} graph edge does not belong to k^{th} basic graph cycle $\left(\mathbf{R}_j^{\varsigma} \bigcap \mathbf{\Gamma}_k^{\varsigma} = \varnothing \right)$.

2.2.2. Resolving equations relating to distribution of shear forces flows taken along closed contours for an arbitrary section of a thin-walled bar

Each j^{th} edge $\mathbf{R}_j^{\varsigma}$, $j = \overline{1, n_r}$ of the graph $\mathbf{G}^{\varsigma}$ corresponds to a constant – *edge weight*, $\forall \kappa : \vec{s}_{\kappa}^{\varsigma} \in \mathbf{R}_j^{\varsigma} \wedge \vec{s}_{\kappa}^{\varsigma} \in \mathbf{S}^{\varsigma}$:

$$p_j = \int\limits_{\ell_{rj}} \frac{d\varsigma}{\delta(\varsigma)} = \sum_{r=1}^{n_{\varsigma rj}} \int\limits_{\ell_{\varsigma} \in \mathbf{R}_j^{\varsigma}} \frac{d\varsigma}{\delta(\varsigma)} = \sum_{r=1}^{n_{\varsigma rj}} \frac{1}{\delta_{\kappa}^{\varsigma}} \int\limits_{\varsigma_{\kappa}}^{\varsigma_{\kappa+1}} d\varsigma = \sum_{r=1}^{n_{\varsigma rj}} \frac{l_{\kappa}^{\varsigma}}{\delta_{\kappa}^{\varsigma}}. \tag{2.1}$$

Let us also compose the *weighting matrix of unbranched sectional parts* (edges of graph $\mathbf{G}^{\varsigma}$) – a square matrix $\mathbf{W}$ with dimensions $n_r \times n_r$ and diagonal elements p_j, $j = \overline{1, n_r}$:

$$\mathbf{W} = \begin{bmatrix} p_1 & 0 & \dots & 0 \\ 0 & p_2 & \dots & 0 \\ \vdots & \vdots & \ddots & \vdots \\ 0 & 0 & 0 & p_{n_r} \end{bmatrix}. \tag{2.2}$$

Besides, each j^{th} graph edge $\mathbf{R}_j^{\varsigma}$ corresponds to the increment of the sectorial coordinate $\mathbf{\Delta\omega}_{\mathbf{r}}^{\varsigma} = \left\{ \Delta\omega_{r,j}^{\varsigma} \mid j = \overline{1, n_r} \right\}^T$, $\forall \kappa : \vec{s}_{\kappa}^{\varsigma} \in \mathbf{R}_j^{\varsigma} \wedge \vec{s}_{\kappa}^{\varsigma} \in \mathbf{S}^{\varsigma}$:

$$\Delta\omega_{r,j}^{\varsigma} = \int\limits_{\ell_{rj}} \rho d\varsigma = \int\limits_{\ell_{rj}} d\omega = \sum_{r=1}^{n_{\varsigma rj}} \int\limits_{\ell_{\varsigma} \in \mathbf{R}_j^{\varsigma}} d\omega = \sum_{r=1}^{n_{\varsigma rj}} \int\limits_{\varsigma_{\kappa}}^{\varsigma_{\kappa+1}} d\omega = \sum_{r=1}^{n_{\varsigma rj}} \Delta\omega_{\kappa}^{\varsigma}. \tag{2.3}$$

Each closed contour of the section $\mathbf{\Gamma}_k^{r\varsigma}$, $k=\overline{1,n_k}$, corresponds to the following constant – *contour weight*, $f_{kj} \in \mathbf{F}$, $\forall j : \mathbf{R}_j^{\varsigma} \subseteq \mathbf{\Gamma}_k^{r\varsigma}$:

$$\tilde{p}_k = \oint\limits_{\Gamma_k^{r\varsigma}} \frac{d\varsigma}{\delta(\varsigma)} = \int\limits_{\mathrm{R}_j^{\varsigma} \subseteq \Gamma_k^{r\varsigma}} \frac{d\varsigma}{\delta(\varsigma)} = \sum_{j=1}^{n_{r\varsigma\Gamma k}} \left| f_{kj} \right| p_j. \tag{2.4}$$

Let us also introduce the *weighting matrix of sectional contours* – a square matrix $\mathbf{K}$ with dimensions $n_k \times n_k$:

$$\mathrm{K} = \begin{bmatrix} \tilde{p}_{11} & -p_{12} & \cdots & -p_{1k} & \cdots & -p_{1n_k} \\ -p_{21} & \tilde{p}_{22} & \cdots & -p_{2k} & \cdots & -p_{2n_k} \\ \vdots & \vdots & \ddots & \vdots & \vdots & \vdots \\ -p_{k1} & -p_{k2} & \cdots & \tilde{p}_{kk} & \cdots & -p_{kn_k} \\ \vdots & \vdots & \vdots & \vdots & \ddots & \vdots \\ -p_{n_k 1} & -p_{n_k 2} & \cdots & -p_{n_k k} & \cdots & \tilde{p}_{n_k n_k} \end{bmatrix}, \tag{2.5}$$

where the diagonal elements of the matrix are the weights of k^{th} closed contour, $\tilde{p}_{kk} = \tilde{p}_k$, $k=\overline{1,n_k}$; other elements of the matrix $p_{\alpha\beta}$ take zero value $p_{\alpha\beta} = p_{\beta\alpha} = 0$ when corresponded closed contours have no common edges: $\Gamma_{\alpha}^{\varsigma} \bigcap \Gamma_{\beta}^{\varsigma} = \varnothing$, and the sum of the weights for all common edges: $p_{\alpha\beta} = p_{\beta\alpha} = \sum\limits_r p_r, \forall r \ : \ \mathrm{R}_r^{\varsigma} \subseteq \Gamma_{\alpha}^{\varsigma} \wedge \mathrm{R}_r^{\varsigma} \subseteq \Gamma_{\beta}^{\varsigma}$.

Let us consider the problem of torsion for an arbitrary thin-walled section subjected to total torque M_x only. When the cross-section consists of a certain number of closed (connected and/or disconnected) contours, as well as open parts, the torsion problem for the cross-section of the thin-walled bar is statically indeterminate. Therefore, not only static equations but also strain compatibility conditions must be introduced to consideration.

Let us formulate the strain compatibility conditions considering Castigliano's functional. The latter can be identified with an expression for strain energy formulated in terms of stresses for an isotropic material [5]:

$$\mathrm{C} = \frac{1}{2G}\left(\sum_{j=1}^{n_r} \left(\int\limits_{\ell_j} \frac{\left(\sigma(\varsigma)\right)^2}{2(1+\nu)} \delta(\varsigma)\, d\varsigma + \int\limits_{\ell_j} \left(\tau(\varsigma)\right)^2 \delta(\varsigma)\, d\varsigma \right) \right). \tag{2.6}$$

Besides, normal stresses $\sigma(\varsigma)$ can be omitted, as total torque acts only:

$$\mathrm{C} = \frac{1}{2G}\left(\sum_{j=1}^{n_r} \int\limits_{\ell_j} \left(\tau(\varsigma)\right)^2 \delta(\varsigma)\, d\varsigma \right). \tag{2.7}$$

Let us rewrite Castigliano's functional $\mathbf{C}$ Equation (2.7) substituting shear stresses $\tau(\varsigma)$ by their representation in terms of contour flows $\tilde{\vec{T}} = \left\{\tilde{T}_k\right\}^T$, $k=\overline{1,n_k}$:

$$\tilde{\tau}_k(\varsigma) = \frac{\tilde{T}_k(\varsigma)}{\delta_k(\varsigma)}. \tag{2.8}$$

In this case we obtain the following expression for Castigliano's functional:

$$\begin{aligned} \mathrm{C} = {} & \frac{\tilde{T}_1^2}{2G} \oint\limits_{\Gamma_1} \frac{d\varsigma}{\delta(\varsigma)} + \frac{\tilde{T}_2^2}{2G} \oint\limits_{\Gamma_2} \frac{d\varsigma}{\delta(\varsigma)} + \ldots + \frac{\tilde{T}_k^2}{2G} \oint\limits_{\Gamma_k} \frac{d\varsigma}{\delta(\varsigma)} - \frac{\tilde{T}_1 \tilde{T}_2}{G} \int\limits_{\Gamma_{12}} \frac{d\varsigma}{\delta(\varsigma)} - \frac{\tilde{T}_1 \tilde{T}_3}{G} \int\limits_{\Gamma_{13}} \frac{d\varsigma}{\delta(\varsigma)} - \ldots \\ \ldots - {} & \frac{\tilde{T}_1 \tilde{T}_k}{G} \int\limits_{\Gamma_{1k}} \frac{d\varsigma}{\delta(\varsigma)} - \frac{\tilde{T}_2 \tilde{T}_3}{G} \int\limits_{\Gamma_{23}} \frac{d\varsigma}{\delta(\varsigma)} - \frac{\tilde{T}_2 \tilde{T}_4}{G} \int\limits_{\Gamma_{24}} \frac{d\varsigma}{\delta(\varsigma)} - \ldots - \frac{\tilde{T}_2 \tilde{T}_k}{G} \int\limits_{\Gamma_{2k}} \frac{d\varsigma}{\delta(\varsigma)} - \ldots - \frac{\tilde{T}_{k-1} \tilde{T}_k}{G} \int\limits_{\Gamma_{k-1,k}} \frac{d\varsigma}{\delta(\varsigma)}. \end{aligned} \tag{2.9}$$

Negative summands $\frac{\tilde{T}_{k-1}\tilde{T}_k}{G}\int\limits_{\Gamma_{k-1,k}}\frac{d\varsigma}{\delta(\varsigma)}$ in Equation (2.9) take into account the mutual work of the counter flows of shear stresses on the common parts of the thin-walled bar cross-section.

It is evident that the resulting torsional moment in the section caused by all contour flows of shear stresses $\vec{\tilde{T}}=\left\{\tilde{T}_k\right\}^T$, $k=\overline{1,n_k}$ equals to the sum of the torsional moments caused by each of these flows [5]:

$$M_x=\sum_{k=1}^{n_k}\tilde{T}_k\Omega_k, \tag{2.10}$$

where Ω_k is the double area embraced by k^{th} closed contour Γ_k^{ς} of the section.

Let us present the formulated problem in the form of a mathematical programming task, namely as a problem for unknown contour shear forces flows $\vec{\tilde{T}}=\left\{\tilde{T}_k\right\}^T$, $k=\overline{1,n_k}$ that ensure the least value of the optimum criterion, i.e. Castigliano's functional $\mathbf{C}$ Equation (2.9) subject to equilibrium condition Equation (2.10).

Let us present the solution of the formulated problem as follow:

$$\tilde{T}_k=\tilde{a}_k\frac{M_x}{\Omega_0}, \tag{2.11}$$

where Ω_0 is the double area for all closed contours of the section $\mathbf{\Phi}^{\varsigma}$, $\Omega_0=\sum_{k=1}^{n_k}\Omega_k$; $\tilde{a}_k$ is the factor for the distribution of shear forces flows along k^{th} closed contour. Then Castigliano's functional Equation (2.9) can be rewritten as presented below:

$$\begin{aligned}\mathrm{C}=\frac{M_x^2}{2G\Omega_0^2}\Bigg(&\tilde{a}_1^2\oint\limits_{\Gamma_1}\frac{d\varsigma}{\delta(\varsigma)}+\tilde{a}_2^2\oint\limits_{\Gamma_2}\frac{d\varsigma}{\delta(\varsigma)}+\ldots+\tilde{a}_k^2\oint\limits_{\Gamma_k}\frac{d\varsigma}{\delta(\varsigma)}-2\tilde{a}_1\tilde{a}_2\int\limits_{\Gamma_{12}}\frac{d\varsigma}{\delta(\varsigma)}-2\tilde{a}_1\tilde{a}_2\int\limits_{\Gamma_{12}}\frac{d\varsigma}{\delta(\varsigma)}-\\&-2\tilde{a}_1\tilde{a}_3\int\limits_{\Gamma_{13}}\frac{d\varsigma}{\delta(\varsigma)}-\ldots-2\tilde{a}_1\tilde{a}_k\int\limits_{\Gamma_{1k}}\frac{d\varsigma}{\delta(\varsigma)}-2\tilde{a}_2\tilde{a}_3\int\limits_{\Gamma_{23}}\frac{d\varsigma}{\delta(\varsigma)}-\ldots\\&\ldots-2\tilde{a}_2\tilde{a}_4\int\limits_{\Gamma_{24}}\frac{d\varsigma}{\delta(\varsigma)}-2\tilde{a}_2\tilde{a}_k\int\limits_{\Gamma_{2k}}\frac{d\varsigma}{\delta(\varsigma)}-\ldots-2\tilde{a}_{k-1}\tilde{a}_k\int\limits_{\Gamma_{k-1,k}}\frac{d\varsigma}{\delta(\varsigma)}\Bigg),\end{aligned} \tag{2.11}$$

and the equilibrium equation Equation (2.10) can be presented by the following:

$$M_x=\sum_{k=1}^{n_k}\tilde{a}_k\frac{M_x}{\Omega_0}\Omega_k=\frac{M_x}{\Omega_0}\sum_{k=1}^{n_k}\tilde{a}_k\Omega_k$$

or

$$\Omega_0=\sum_{k=1}^{n_k}\tilde{a}_k\Omega_k. \tag{2.12}$$

So, the formulated problem can be presented as a searching problem for unknown distribution factors $\vec{\tilde{a}}=\left\{\tilde{a}_k\right\}^T$, $k=\overline{1,n_k}$ of shear forces flows taken along closed contours of section that ensure the least value of Castigliano's functional $\mathbf{C}$ Equation (2.11) subject to equilibrium condition Equation (2.12).

The method of Lagrange multipliers can be used to reduce the problem Equations (2.11)–(2.12) to the searching for a stationary point of the following modified functional $\Lambda\left(\vec{\tilde{a}},\lambda_a\right)$, where λ_a is the Lagrange multiplier. Besides, the stationary conditions for the modified functional $\Lambda\left(\vec{\tilde{a}},\lambda_a\right)$ can be transformed to a system of linear algebraic equations with an order of n_k+1 presented below in the vector-matrix form:

$$\begin{Vmatrix}\mathrm{K} & \vec{\Omega}\\ \left(\vec{\Omega}\right)^T & 0\end{Vmatrix}\times\begin{Vmatrix}\vec{\tilde{a}}\\ \lambda_a\end{Vmatrix}=\begin{Vmatrix}0_k\\ \Omega_0\end{Vmatrix}, \tag{2.13}$$

where $\vec{\Omega} = \{\Omega_k\}^T$, $k = \overline{1, n_k}$ is the column vector of double areas embraced by the closed contours of the thin-walled bar. The resolving system of equations Equation (2.13) to calculate distribution factors $\vec{\tilde{a}}_k = \{\tilde{a}_k\}^T$, $k = \overline{1, n_k}$ of shear forces flows along the closed contours of the section is presented below:

$$\begin{bmatrix} \tilde{p}_{11} & -p_{12} & \cdots & -p_{1k} & \cdots & -p_{1n_k} & \Omega_1 \\ -p_{21} & \tilde{p}_{22} & \cdots & -p_{2k} & \cdots & -p_{2n_k} & \Omega_2 \\ \vdots & \vdots & \ddots & \vdots & \vdots & \vdots & \vdots \\ -p_{k1} & -p_{k2} & \cdots & \tilde{p}_{kk} & \cdots & -p_{kn_k} & \Omega_k \\ \vdots & \vdots & \vdots & \vdots & \ddots & \vdots & \vdots \\ -p_{n_k 1} & -p_{n_k 2} & \cdots & -p_{n_k k} & \cdots & \tilde{p}_{n_k n_k} & \Omega_{n_k} \\ \Omega_1 & \Omega_2 & \cdots & \Omega_k & \cdots & \Omega_{n_k} & 0 \end{bmatrix} \times \begin{bmatrix} \tilde{a}_1 \\ \tilde{a}_2 \\ \vdots \\ \tilde{a}_k \\ \vdots \\ \tilde{a}_{n_k} \\ \lambda_a \end{bmatrix} = \begin{bmatrix} 0 \\ 0 \\ \vdots \\ 0 \\ \vdots \\ 0 \\ \Omega_0 \end{bmatrix}, \quad (2.14)$$

where the diagonal elements of the matrix are the weights of k^{th} closed contour,

$\tilde{p}_{kk} = \tilde{p}_k$, $k = \overline{1, n_k}$; Ω_k is double area embraced by k^{th} closed contour Γ_k^{ς}, $\Omega_0 = \sum_{k=1}^{n_k} \Omega_k$;

λ_a is the Lagrange multiplier. Other elements of the matrix $p_{\alpha\beta}$ take zero value $p_{\alpha\beta} = p_{\beta\alpha} = 0$ when corresponded closed contours have no common edges: $\Gamma_\alpha^{\varsigma} \bigcap \Gamma_\beta^{\varsigma} = \varnothing$, and the sum of weights for all common edges [5] is $p_{\alpha\beta} = p_{\beta\alpha} = \sum_r p_r, \forall r \ : \ \mathrm{R}_r^{\varsigma} \subseteq \Gamma_\alpha^{\varsigma} \wedge \mathrm{R}_r^{\varsigma} \subseteq \Gamma_\beta^{\varsigma}$.

The solution of the system of algebraic equations Equation (2.14) returns the column vector of factors $\vec{\tilde{a}}_k = \left\{\tilde{a}_k \mid k = \overline{1, n_k}\right\}$ for the distribution of shear forces flows along the closed contours of the section. Based on $\vec{\tilde{a}}_k$, we can generate the column vector of factors for the distribution of shear forces flows along the graph $\mathbf{G}^{\varsigma}$ edges: $\mathrm{A}_r = \left\{a_j \mid j = \overline{1, n_r}\right\}$, where each element should be determined as:

$$a_j = \sum_{k=1}^{n_k} f_{kj} \tilde{a}_k, \quad f_{kj} \in \mathbf{F} \ \forall j = \overline{1, n_r}, \quad (2.15)$$

Since every graph edge $\mathbf{R}_j^{\varsigma}$, $j = \overline{1, n_r}$, is described by the set of sectional segments $\vec{s}_r^{\varsigma} \in \mathrm{S}^{\varsigma}$ as: $\mathrm{R}_j^{\varsigma} = \{\vec{s}_r^{\varsigma} : \vec{s}_r^{\varsigma} \in \mathrm{S}^{\varsigma} \wedge \vec{s}_r^{\varsigma} \in \mathrm{R}_j \mid r = \overline{1, n_{\varsigma rj}}\}$, then it is possible to determine for each sectional segment $\vec{s}_\kappa^{\varsigma} \in \mathrm{S}^{\varsigma}$ the value of piecewise constant *distribution function for shear flows taken along section* $a^{\varsigma}(\varsigma)$ as the set of $\mathrm{a}^{\varsigma} = \left\{a_\kappa^{\varsigma} \mid \kappa = \overline{1, n_\varsigma - 1}\right\}$ as follows: $a_\kappa^{\varsigma} = a_j$, $\forall \kappa : \vec{s}_\kappa^{\varsigma} \bigcap \Phi^{\varsigma} \neq \varnothing$, and $a_\kappa^{\varsigma} = 0$, otherwise.

2.3. Resolving equations for an arbitrary cross-section of a thin-walled bar

The search problem of shear forces flows for an arbitrary cross-section of a thin-walled bar (including open-closed multi-contour cross-sections) can be transformed into a minimization problem of Castigliano's functional $\mathbf{C}$ subject to constraints-equalities of shear forces flows equilibrium formulated for cross-section branch points, as well as subject to equilibrium equation for the whole cross-section relating to longitudinal axes of the thin-walled bar [5].

Let us present the formulated problem as a mathematical programming task, namely as searching for unknown values of shear forces flows at the start points of unbranched parts of a section:

$$\vec{T}_S = \left\{T_{S,j}\right\}^T, \ j = \overline{1, n_r}, \quad (3.1)$$

which ensure the least value of the optimum criterion – Castigliano's functional $\mathbf{C}$:

$$\mathrm{C}^* = \mathrm{C}(\vec{T}_S^{\,*}) = \min_{\vec{T}_S \in \Im_T} \mathrm{C}\left(\vec{T}_S\right) \quad (3.2)$$

on a hyperplane of feasible decisions $\Im_T$ described by the following system of constraints-equalities:

$$\begin{cases} \mathrm{f}\left(\vec{T}_S\right) = \left\{ f_v\left(\vec{T}_S\right) = 0 \,|\, v = \overline{1, n_v - 1} \right\}; \\ f_x\left(\vec{T}_S\right) = 0, \end{cases} \tag{3.3}$$

where $\vec{T}_S$ is the vector of design variables (searched shear flows);

n_r is the number of unknown shear flows;

$\vec{T}_S^{\,*}$ is the optimum decision of the problem;

$\mathbf{C}^*$ is the minimum value of Castigliano's functional;

f_v is the function of the vector argument $\vec{T}_S$;

n_v is the general number of constraints-equalities $f_v\left(\vec{T}_S\right)$ and $f_x\left(\vec{T}_S\right)$ which define the hyperplane of feasible decisions $\Im_T$ in the sought space.

For Castigliano's functional $\mathbf{C}$ we will consider only those Euler's equations that define the strain compatibility conditions and are expressed depending on shear forces flows $\vec{T}_S = \left\{T_{S,j}\right\}^T$, $j = \overline{1, n_r}$. Let us rewrite Castigliano's functional $\mathbf{C}$ Equation (2.6) replacing normal stresses $\sigma(\varsigma)$ by Equation (1.1), and shear stresses $\tau(\varsigma)$ – by the dependence on shear forces flows Equation (1.2) as presented below:

$$\tau_j\left(\varsigma\right) = \frac{1}{\delta_j\left(\varsigma\right)}\left(T_{S,j} - \frac{Q_z}{I_y} S_{oy,j}\left(\varsigma\right) - \frac{Q_y}{I_z} S_{oz,j}\left(\varsigma\right) - \frac{M_\varpi}{I_\varpi} S_{o\varpi,j}\left(\varsigma\right) \right); \tag{3.4}$$

$$\begin{aligned} \mathrm{C} = \frac{1}{2G}\Bigg(\Bigg(\sum_{j=1}^{n_r} \Bigg(\int_{\ell_j} \frac{1}{2\left(1+\nu\right)} \left(\frac{N}{A} + \frac{M_y}{I_y} z_j + \frac{M_z}{I_z} y_j + \frac{B}{I_\varpi} \varpi_j \right)^2 \delta_j d\varsigma + \\ + \int_{\ell_j} \left(T_{S,j}^2 - 2T_{S,j} \frac{Q_z}{I_y} S_{oy,j} - 2T_{S,j} \frac{Q_y}{I_z} S_{oz,j} - 2T_{S,j} \frac{M_\varpi}{I_\varpi} S_{o\varpi,j} \right) \frac{d\varsigma}{\delta_j} + \\ + \int_{\ell_j} \left(\frac{Q_z}{I_y} S_{oy,j} + \frac{Q_y}{I_z} S_{oz,j} + \frac{M_\varpi}{I_\varpi} S_{o\varpi,j} \right)^2 \frac{d\varsigma}{\delta_j} \Bigg) \Bigg) \Bigg), \end{aligned} \tag{3.5}$$

where the functional dependence on the angular position ς is omitted to simplify the presented formulas.

Let us leave in Equation (3.5) those summands that depend on shear forces flows values $\vec{T}_S = \left\{T_{S,j}\right\}^T$, $j = \overline{1, n_r}$, and also denote by the symbol … all other summands that do not depend on the vector $\vec{T}_S$. In this way we can obtain Castigliano's functional $\mathbf{C}$ in terms of shear forces flows $\vec{T}_S = \left\{T_{S,j}\right\}^T$ [5] as presented below:

$$\mathrm{C} = \sum_{j=1}^{n_r} \left(\int_{\ell_j} \left(\frac{T_{S,j}^2}{2G} - T_{S,j} \frac{Q_z}{GI_y} S_{oy,j} - T_{S,j} \frac{Q_y}{GI_z} S_{oz,j} - T_{S,j} \frac{M_\varpi}{GI_\varpi} S_{o\varpi,j} \right) \frac{d\varsigma}{\delta_j} + \ldots \right); \tag{3.6}$$

$$\mathrm{C} = \sum_{j=1}^{n_r} \left(\frac{T_{S,j}^2}{2G} \int_{\ell_j} \frac{d\varsigma}{\delta_j} - T_{S,j} \frac{Q_z}{GI_y} \int_{\ell_j} S_{oy,j} \frac{d\varsigma}{\delta_j} - T_{S,j} \frac{Q_y}{GI_z} \int_{\ell_j} S_{oz,j} \frac{d\varsigma}{\delta_j} - T_{S,j} \frac{M_\varpi}{GI_\varpi} \int_{\ell_j} S_{o\varpi,j} \frac{d\varsigma}{\delta_j} + \ldots \right), \tag{3.7}$$

where the integral $\int_{\ell_j} \frac{d\varsigma}{\delta_j}$ can be calculated according to Equation (2.1), and the integrals $\int_{\ell_j} S_{oy,j} \frac{d\varsigma}{\delta_j}$, $\int_{\ell_j} S_{oz,j} \frac{d\varsigma}{\delta_j}$ and $\int_{\ell_j} S_{o\varpi,j} \frac{d\varsigma}{\delta_j}$ – using following Equations (3.8)–(3.10), respectively, $\forall \kappa : \vec{s}_\kappa^{\,\varsigma} \in \mathrm{R}_j^{\varsigma} \wedge \vec{s}_\kappa^{\,\varsigma} \in \mathrm{S}^{\varsigma}$;

$$S_{hz,j} = \int_{\ell_{rj}} \frac{S_{oz,j}^{\varsigma}(\varsigma)d\varsigma}{\delta(\varsigma)} = \sum_{\kappa=1}^{n_{\varsigma rj}} \left(\frac{l_\kappa^{\varsigma}}{6\delta_\kappa^{\varsigma}} \left(S_{oz,\kappa}^{\varsigma,start} + 4S_{oz,\kappa}^{\varsigma,mid} + S_{oz,\kappa}^{\varsigma,end} \right) \right); \tag{3.8}$$

$$S_{hy,j} = \int_{\ell_{rj}} \frac{S_{oy,j}^{\varsigma}(\varsigma)d\varsigma}{\delta(\varsigma)} = \sum_{\kappa=1}^{n_{\varsigma rj}} \left(\frac{l_\kappa^{\varsigma}}{6\delta_\kappa^{\varsigma}} \left(S_{oy,\kappa}^{\varsigma,start} + 4S_{oy,\kappa}^{\varsigma,mid} + S_{oy,\kappa}^{\varsigma,end} \right) \right); \tag{3.9}$$

$$S_{h\varpi,j} = \int_{\ell_{rj}} \frac{S_{o\varpi,j}^{\varsigma}(\varsigma)d\varsigma}{\delta(\varsigma)} = \sum_{\kappa=1}^{n_{\varsigma rj}} \left(\frac{l_\kappa^{\varsigma}}{6\delta_\kappa^{\varsigma}} \left(S_{o\varpi,\kappa}^{\varsigma,start} + 4S_{o\varpi,\kappa}^{\varsigma,mid} + S_{o\varpi,\kappa}^{\varsigma,end} \right) \right). \tag{3.10}$$

Let us define the following column vectors consisting of n_r elements, $\forall j = \overline{1, n_r}$ (according to the number of edges of the graph $\mathbf{G}$):

$$\vec{S}_{hz} = \begin{bmatrix} S_{hz,1} \\ S_{hz,2} \\ \vdots \\ S_{hz,n_r} \end{bmatrix}; \quad \vec{S}_{hy} = \begin{bmatrix} S_{hy,1} \\ S_{hy,2} \\ \vdots \\ S_{hy,n_r} \end{bmatrix}; \quad \vec{S}_{h\omega} = \begin{bmatrix} S_{h\omega,1} \\ S_{h\omega,2} \\ \vdots \\ S_{h\omega,n_r} \end{bmatrix}. \tag{3.11}$$

Using the weighting matrix of unbranched sectional parts $\mathbf{W}$, Equation (2.2), as well as column vectors $\vec{S}_{hz}$, $\vec{S}_{hy}$ and $\vec{S}_{h\varpi}$, Equation (3.11), we can rewrite Castigliano's functional, Equation (3.7), as the following vector-matrix equation:

$$\mathrm{C} = \frac{1}{2G} \vec{T}_S^{\,T} \mathrm{W} \vec{T}_S - \vec{T}_S^{\,T} \frac{Q_y}{GI_z} \vec{S}_{hz} - \vec{T}_S^{\,T} \frac{Q_z}{GI_y} \vec{S}_{hy} - \vec{T}_S^{\,T} \frac{M_\varpi}{GI_\varpi} \vec{S}_{h\varpi} + \ldots \tag{3.12}$$

Next, for each section branch point we can develop an equation of shear forces flows equilibrium in terms of projections on the longitudinal axis of the thin-walled bar. In order to obtain the general view for these equations (the system of equations by the number of branch points in the section), we can use the incidence matrices $\dot{\mathbf{I}}$ and $|\dot{\mathbf{I}}|$ introduced above, which reflect the topological structure of the considered cross-section of the thin-walled bar. In this case we obtain the following system of equations presented below in the matrix-vector form:

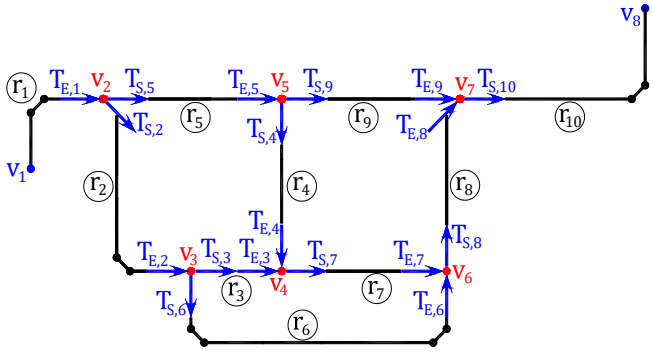

Figure 5. Relating to formulate equilibrium equations for shear stresses flows in branch points of a thin-walled bar.

$$\left(\left| \dot{\mathbf{I}} \right| + \dot{\mathbf{I}} \right) \vec{T}_S - \left(\left| \dot{\mathbf{I}} \right| - \dot{\mathbf{I}} \right) \vec{T}_E = \mathbf{0}, \tag{3.13}$$

where $\vec{T}_S = \left\{ T_{S,j} \right\}^T$, $j = \overline{1, n_r}$ is the vector of shear forces flows at the start points of unbranched sectional parts;

$\vec{T}_E = \left\{T_{E,j}\right\}^T$, $j = \overline{1, n_r}$ is the vector of shear forces flows at the end points of unbranched sectional parts:

$$\vec{T}_E = \vec{T}_S - \Delta\vec{T}, \tag{3.14}$$

where $\Delta\vec{T} = \left\{\Delta T_j\right\}^T$, $j = \overline{1, n_r}$ is the vector of shear forces flows increments for each unbranched sectional part:

$$\Delta\vec{T}_j = \frac{Q_y}{I_z}\vec{S}_{z,j} + \frac{Q_z}{I_y}\vec{S}_{y,j} + \frac{M_\varpi}{I_\varpi}\vec{S}_{\varpi,j}; \tag{3.15}$$

where the vectors $\vec{S}_{z,j}, \vec{S}_{y,j}, \vec{S}_{\varpi,j}$ are presented below:

$$\vec{S}_z = \begin{bmatrix} S_{z,1} \\ S_{z,2} \\ \vdots \\ S_{z,n_r} \end{bmatrix}; \quad \vec{S}_y = \begin{bmatrix} S_{y,1} \\ S_{y,2} \\ \vdots \\ S_{y,n_r} \end{bmatrix}; \quad \vec{S}_\varpi = \begin{bmatrix} S_{\varpi,1} \\ S_{\varpi,2} \\ \vdots \\ S_{\varpi,n_r} \end{bmatrix}; \tag{3.16}$$

and the components of vectors $\vec{S}_{z,j}$, $\vec{S}_{y,j}$, $\vec{S}_{\varpi,j}$ can be calculated as follow, $\forall\kappa : \vec{s}_\kappa^{\,\varsigma} \in \mathrm{R}_j^\varsigma \wedge \vec{s}_\kappa^{\,\varsigma} \in \mathrm{S}^\varsigma$:

$$S_{z,j} = \int\limits_{\ell_{rj}} y^\varsigma(\varsigma)\delta(\varsigma)d\varsigma = \sum_{\kappa=1}^{n_{\varsigma rj}}\left(\delta_\kappa^\varsigma l_\kappa^\varsigma\left(y_\kappa^{\varsigma,start} + \frac{1}{2}\Delta y_\kappa^\varsigma\right)\right); \tag{3.17}$$

$$S_{y,j} = \int\limits_{\ell_{rj}} z^\varsigma(\varsigma)\delta(\varsigma)d\varsigma = \sum_{\kappa=1}^{n_{\varsigma rj}}\left(\delta_\kappa^\varsigma l_\kappa^\varsigma\left(z_\kappa^{\varsigma,start} + \frac{1}{2}\Delta z_\kappa^\varsigma\right)\right); \tag{3.18}$$

$$S_{\varpi,j} = \int\limits_{\ell_{rj}} \varpi^\varsigma(\varsigma)\delta(\varsigma)d\varsigma = \sum_{\kappa=1}^{n_{\varsigma rj}}\left(\delta_\kappa^\varsigma l_\kappa^\varsigma\left(\varpi_\kappa^{\varsigma,start} + \frac{1}{2}\Delta\varpi_\kappa^\varsigma\right)\right). \tag{3.19}$$

Let us rewrite the system of equations Equation (3.13) substituting $\vec{T}_E$ according to Equation (3.14). We obtain the following system of equations:

$$\left(\left|\dot{\mathbf{I}}\right| + \dot{\mathbf{I}}\right)\vec{T}_S - \left(\left|\dot{\mathbf{I}}\right| - \dot{\mathbf{I}}\right) \times \left(\vec{T}_S - \Delta\vec{T}\right) = \mathbf{0}; \tag{3.20}$$

$$\left(\left|\dot{\mathbf{I}}\right| - \dot{\mathbf{I}}\right)\vec{T}_S - \left(\left|\dot{\mathbf{I}}\right| - \dot{\mathbf{I}}\right)\vec{T}_S + \left(\left|\dot{\mathbf{I}}\right| - \dot{\mathbf{I}}\right)\Delta\vec{T} = \mathbf{0}; \tag{3.21}$$

$$2\dot{\mathbf{I}}\vec{T}_S + \left(\left|\dot{\mathbf{I}}\right| - \dot{\mathbf{I}}\right)\Delta\vec{T} = \mathbf{0}; \tag{3.22}$$

and taking into account Equaton (3.15):

$$2\dot{\mathbf{I}}\vec{T}_S + \left(\left|\dot{\mathbf{I}}\right| - \dot{\mathbf{I}}\right) \times \left(\frac{Q_y}{I_z}\vec{S}_{z,j} + \frac{Q_z}{I_y}\vec{S}_{y,j} + \frac{M_\varpi}{I_\varpi}\vec{S}_{\varpi,j}\right) = \mathbf{0}. \tag{3.23}$$

The system of equations in Equation (3.23) in the matrix-vector form has n_v equilibrium equations. The last equation is linear-dependent or a linear combination from the previous $n_v - 1$ equations. Let us rewrite Equation (3.23) excluding the last equilibrium equation:

$$2\dot{\mathbf{I}}'\vec{T}_S + \left(\left|\dot{\mathbf{I}}'\right| - \dot{\mathbf{I}}'\right) \times \left(\frac{Q_y}{I_z}\vec{S}_{z,j} + \frac{Q_z}{I_y}\vec{S}_{y,j} + \frac{M_\varpi}{I_\varpi}\vec{S}_{\varpi,j}\right) = \mathbf{0}; \tag{3.24}$$

where $\dot{\mathrm{I}}'$ is the incidence matrix of the graph $\mathbf{G}^{\circ}$ truncated by the last row with dimensions $\left(n_v - 1\right) \times n_r$, $\dot{\mathrm{I}}' = \left\{g_{ij} \mid i = \overline{1, n_v - 1},\ j = \overline{1, n_r}\right\}$;

$\left|\dot{\mathrm{I}}'\right|$ is the matrix composed using the modulus of elements g_{ij} of the truncated matrix $\dot{\mathrm{I}}'$ as $\left|\dot{\mathrm{I}}'\right| = \left\{\left|g_{ij}\right| \mid i = \overline{1, n_v - 1},\ j = \overline{1, n_r}\right\}$.

It is possible to derive the last equilibrium equation relating to the longitudinal axis $x - x$ of the thin-walled bar as a condition of the static equivalence of the torsion moment caused by the shear forces flows to the total torque M_x acting in the cross-section of the thin-walled bar:

$$M_x - \sum_{j=1}^{n_r} \int_{\ell_j} T_j(\varsigma)\, d\omega = 0; \tag{3.25}$$

where $T_j(\varsigma)$ is the shear forces flow at some point of the cross-section, which can be expressed depending on shear forces flow $T_{S,j}(\varsigma)$ at the start point of the corresponded unbranched part of the section as follow:

$$T_j = T_{S,j} - \frac{Q_y}{I_z} S_{oz,j} - \frac{Q_z}{I_y} S_{oy,j} - \frac{M_\varpi}{I_\varpi} S_{o\varpi,j}, \tag{3.26}$$

where we omitted the functional dependence from the angular position ς (to simplify presented formulas).

Then:

$$M_x - \sum_{j=1}^{n_r} \int_{\ell_j} \left(T_{S,j} - \frac{Q_y}{I_z} S_{oz,j} - \frac{Q_z}{I_y} S_{oy,j} - \frac{M_\varpi}{I_\varpi} S_{o\varpi,j} \right) \rho d\varsigma = 0;$$

$$M_x - \sum_{j=1}^{n_r} \left(T_{S,j} \int_{\ell_j} \rho d\varsigma - \frac{Q_y}{I_z} \int_{\ell_j} S_{oz,j} \rho d\varsigma - \frac{Q_z}{I_y} \int_{\ell_j} S_{oy,j} \rho d\varsigma - \frac{M_\varpi}{I_\varpi} \int_{\ell_j} S_{o\varpi,j} \rho d\varsigma \right) = 0.$$

Finally, we obtain [5]:

$$\sum_{j=1}^{n_r} T_{S,j} \int_{\ell_j} \rho d\varsigma - \frac{Q_y}{I_z} \sum_{j=1}^{n_r} \int_{\ell_j} S_{oz,j} \rho d\varsigma - \frac{Q_z}{I_y} \sum_{j=1}^{n_r} \int_{\ell_j} S_{oy,j} \rho d\varsigma - \frac{M_\varpi}{I_\varpi} \sum_{j=1}^{n_r} \int_{\ell_j} S_{o\varpi,j} \rho d\varsigma - M_x = 0; \tag{3.27}$$

where integrals $\sum_{j=1}^{n_r} \int_{\ell_j} S_{oz,j} \rho d\varsigma$, $\sum_{j=1}^{n_r} \int_{\ell_j} S_{oy,j} \rho d\varsigma$ and $\sum_{j=1}^{n_r} \int_{\ell_j} S_{o\varpi,j} \rho d\varsigma$ can be calculated using Equations. (3.28)–(3.30), respectively, $\forall \kappa : \vec{s}_\kappa^{\,\varsigma} \in \mathrm{R}_j^{\varsigma} \wedge \vec{s}_\kappa^{\,\varsigma} \in \mathrm{S}^{\varsigma}$:

$$S_{\rho z} = \sum_{j=1}^{n_r} \int_{\ell_{rj}} S_{oz,j}^{\varsigma}(\omega) \rho d\varsigma = \sum_{j=1}^{n_r} \left(\sum_{\kappa=1}^{n_{\varsigma rj}} \frac{\Delta\omega_\kappa^{\varsigma}}{6} \left(S_{oz,\kappa}^{\varsigma,start} + 4S_{oz,\kappa}^{\varsigma,mid} + S_{oz,\kappa}^{\varsigma,end} \right) \right); \tag{3.28}$$

$$S_{\rho y} = \sum_{j=1}^{n_r} \int_{\ell_{rj}} S_{oy,j}^{\varsigma}(\omega) \rho d\varsigma = \sum_{j=1}^{n_r} \left(\sum_{\kappa=1}^{n_{\varsigma rj}} \frac{\Delta\omega_\kappa^{\varsigma}}{6} \left(S_{oy,\kappa}^{\varsigma,start} + 4S_{oy,\kappa}^{\varsigma,mid} + S_{oy,\kappa}^{\varsigma,end} \right) \right); \tag{3.29}$$

$$S_{\rho\varpi} = \sum_{j=1}^{n_r} \int_{\ell_{rj}} S_{o\varpi,j}^{\varsigma}(\omega) \rho d\varsigma = \sum_{j=1}^{n_r} \left(\sum_{\kappa=1}^{n_{\varsigma rj}} \frac{\Delta\omega_\kappa^{\varsigma}}{6} \left(S_{o\varpi,\kappa}^{\varsigma,start} + 4S_{o\varpi,\kappa}^{\varsigma,mid} + S_{o\varpi,\kappa}^{\varsigma,end} \right) \right). \tag{3.30}$$

Let us rewrite the constraints-equality Equation (3.27) using vector representation taking into account Equations (3.28)–(3.30) as presented below:

$$\vec{\omega}^T \vec{T}_S - \frac{Q_y}{I_z} S_{\rho z} - \frac{Q_z}{I_y} S_{\rho y} - \frac{M_\varpi}{I_\varpi} S_{\rho\varpi} - M_x = 0. \tag{3.31}$$

Thus, the formulated problem is presented as a mathematical programming task of searching for the unknown values of shear forces flows at the start points of the unbranched parts of the section:

$$\vec{T}_S = \left\{ T_{S,j} \right\}^T,\ j = \overline{1, n_r}, \tag{3.32}$$

which ensure the least value of the following Castigliano's functional $\mathbf{C}$ Equation (3.12):

$$\mathbf{C} = \frac{1}{2G}\vec{T}_S^T \mathbf{W}\vec{T}_S - \vec{T}_S^T \frac{Q_y}{GI_z}\vec{S}_{hz} - \vec{T}_S^T \frac{Q_z}{GI_y}\vec{S}_{hy} - \vec{T}_S^T \frac{M_\varpi}{GI_\varpi}\vec{S}_{h\varpi} + \ldots \to \min, \tag{3.33}$$

subject to the following equilibrium conditions Equations (3.24) and (3.31):

$$\begin{cases} 2\dot{\mathbf{I}}'\vec{T}_S + \left(\left|\dot{\mathbf{I}}'\right| - \dot{\mathbf{I}}'\right)\left(\frac{Q_y}{I_z}\vec{S}_{z,j} + \frac{Q_z}{I_y}\vec{S}_{y,j} + \frac{M_\varpi}{I_\varpi}\vec{S}_{\varpi,j}\right) = \mathbf{0}; \\ \vec{\omega}^T\vec{T}_S - \frac{Q_y}{I_z}S_{\rho z} - \frac{Q_z}{I_y}S_{\rho y} - \frac{M_\varpi}{I_\varpi}S_{\rho\varpi} - M_x = 0. \end{cases} \tag{3.34}$$

The method of Lagrange multipliers can be used to reduce the mathematical programming task Equations (3.32)–(3.34) to the searching for the stationary point of the following modified functional $\Lambda\left(\vec{T}_S, \vec{\lambda}^T, \lambda_{n_v}\right)$:

$$\begin{aligned} \Lambda\left(\vec{T}_S, \vec{\lambda}^T, \lambda_{n_v}\right) = {} & \frac{1}{2G}\vec{T}_S^T \mathrm{W}\vec{T}_S - \vec{T}_S^T \frac{Q_y}{GI_z}\vec{S}_{hz} - \vec{T}_S^T \frac{Q_z}{GI_y}\vec{S}_{hy} - \vec{T}_S^T \frac{M_\varpi}{GI_\varpi}\vec{S}_{h\varpi} + \\ & + \vec{\lambda}^T\left[2\dot{\mathrm{I}}'\vec{T}_S + \left(\left|\dot{\mathrm{I}}'\right| - \dot{\mathrm{I}}'\right)\left(\frac{Q_y}{I_z}\vec{S}_{z,j} + \frac{Q_z}{I_y}\vec{S}_{y,j} + \frac{M_\varpi}{I_\varpi}\vec{S}_{\varpi,j}\right)\right] + \\ & + \lambda_{n_v}\left[\vec{\omega}^T\vec{T}_S - \frac{Q_y}{I_z}S_{\rho z} - \frac{Q_z}{I_y}S_{\rho y} - \frac{M_\varpi}{I_\varpi}S_{\rho\varpi} - M_x\right] \to \min, \end{aligned} \tag{3.35}$$

where $\vec{\lambda} = \left\{\lambda_f\right\}$, $f = \overline{1, n_v - 1}$ is the vector of Lagrange multipliers consisting of $n_v - 1$ elements;

λ_{n_v} is an additional Lagrange multiplier.

The stationary conditions of the modified functional $\Lambda\left(\vec{T}_S, \vec{\lambda}^T, \lambda_{n_v}\right)$, Equation (3.35), can be transformed into a system of $n_r + n_v$ linear algebraic equations and presented in vector-matrix form as follow [5]:

$$\begin{aligned} & \left\|\begin{bmatrix} \frac{1}{G}\mathbf{W} & 2\dot{\mathbf{I}}'^T & \mathbf{\Delta\omega}_{\mathbf{r}}^{\varsigma} \\ 2\dot{\mathbf{I}}' & \mathbf{\Theta}_{n_v-1,n_v-1} & \mathbf{0}_{n_v-1} \\ \left(\mathbf{\Delta\omega}_{\mathbf{r}}^{\varsigma}\right)^T & \mathbf{0}_{n_v-1}^T & 0 \end{bmatrix}\right\| \times \left\|\begin{bmatrix} \vec{T}_S \\ \vec{\lambda} \\ \lambda_{n_v} \end{bmatrix}\right\| = M_x \times \left\|\begin{bmatrix} \mathbf{0}_{n_r} \\ \mathbf{0}_{n_v-1} \\ 1 \end{bmatrix}\right\| + \frac{Q_y}{I_z} \times \left\|\begin{bmatrix} \frac{\vec{S}_{hz}}{G} \\ \left(\dot{\mathbf{I}}' - \left|\dot{\mathbf{I}}'\right|\right)\vec{S}_z \\ S_{\rho z} \end{bmatrix}\right\| + \\ & + \frac{Q_z}{I_y} \times \left\|\begin{bmatrix} \frac{\vec{S}_{hy}}{G} \\ \left(\dot{\mathbf{I}}' - \left|\dot{\mathbf{I}}'\right|\right)\vec{S}_y \\ S_{\rho y} \end{bmatrix}\right\| + \frac{M_\varpi}{I_\varpi} \times \left\|\begin{bmatrix} \frac{\vec{S}_{h\varpi}}{G} \\ \left(\dot{\mathbf{I}}' - \left|\dot{\mathbf{I}}'\right|\right)\vec{S}_\varpi \\ S_{\rho\varpi} \end{bmatrix}\right\| \end{aligned} \tag{3.36}$$

where

$$\mathbf{M} = \begin{bmatrix} 1/G\,\mathbf{W} & 2\dot{\mathbf{I}}'^T & \mathbf{\Delta\omega}_{\mathbf{r}}^{\varsigma} \\ 2\dot{\mathbf{I}}' & \mathbf{\Theta}_{n_v-1,n_v-1} & \mathbf{0}_{n_v-1} \\ \left(\mathbf{\Delta\omega}_{\mathbf{r}}^{\varsigma}\right)^T & \mathbf{0}_{n_v-1}^T & 0 \end{bmatrix};$$

$\mathbf{M}$ is a square matrix with dimensions $\left(n_r + n_v\right) \times \left(n_r + n_v\right)$, where n_r and n_v are the numbers of edges

and vertices of the graph $\mathbf{G}^{\varsigma}$, respectively; $\mathbf{\Delta\omega}_{\mathrm{r}}^{\varsigma}$ is the column vector of sectorial coordinates increments $\mathbf{\Delta\omega}_{\mathrm{r}}^{\varsigma}=\left\{\Delta\omega_{r,j}^{\varsigma}\mid j=\overline{1,n_r}\right\}^T$ consisting of n_r components calculated according to Equation (2.3); $\vec{S}_y$, $\vec{S}_z$, $\vec{S}_{\varpi}$ are the column vectors Equation (3.16) with n_r components calculated according to Equations (3.17)–(3.19) respectively; $\vec{S}_{hy}, \vec{S}_{hz}, \vec{S}_{h\varpi}$ are the column vectors Equation (3.11) with n_r components calculated according to Equations (3.8)–(3.10), respectively; $S_{\rho y}, S_{\rho z}, S_{\rho\varpi}$ are the integral section properties calculated according to Equations (3.28)–(3.30), respectively.

The solution of the system of equations in Equation (3.36) determines the column vector of shear forces flows $\vec{T}_S=\left\{T_{S,j}\right\}^T$, $j=\overline{1,n_r}$, at the start points of unbranched cross-section parts. The vector $\vec{T}_S$ can be also presented as follow:

$$\vec{T}_S=M_x\vec{b}_x+\frac{Q_y}{I_z}\vec{b}_z+\frac{Q_z}{I_y}\vec{b}_y+\frac{M_{\varpi}}{I_{\varpi}}\vec{b}_{\varpi}. \tag{3.37}$$

In this case, the system of algebraic equations, Equation (3.36), disintegrates and transforms into four systems of n_r+n_v algebraic equations relating to the column vectors $\vec{b}_x, \vec{b}_y, \vec{b}_z$ and $\vec{b}_{\varpi}$ consisting of n_r elements [5] as presented below:

$$\begin{gathered}\mathbf{M}\times\left\|\begin{bmatrix}\vec{b}_x\\ \vec{\lambda}_x\\ \lambda_{n_vx}\end{bmatrix}\right\|=\left\|\begin{bmatrix}\mathbf{0}_{n_r}\\ \mathbf{0}_{n_v-1}\\ 1\end{bmatrix}\right\};\quad \mathbf{M}\times\left\|\begin{bmatrix}\vec{b}_y\\ \vec{\lambda}_y\\ \lambda_{n_vy}\end{bmatrix}\right\|=\left\|\begin{bmatrix}\dfrac{\vec{S}_{hy}}{G}\\ \left(\dot{\mathbf{I}}'-\left|\dot{\mathbf{I}}'\right|\right)\times\vec{S}_y\\ S_{\rho y}\end{bmatrix}\right\};\\ \mathbf{M}\times\left\|\begin{bmatrix}\vec{b}_z\\ \vec{\lambda}_z\\ \lambda_{n_vz}\end{bmatrix}\right\|=\left\|\begin{bmatrix}\dfrac{\vec{S}_{hz}}{G}\\ \left(\dot{\mathbf{I}}'-\left|\dot{\mathbf{I}}'\right|\right)\times\vec{S}_z\\ S_{\rho z}\end{bmatrix}\right\};\quad \mathbf{M}\times\left\|\begin{bmatrix}\vec{b}_{\varpi}\\ \vec{\lambda}_{\varpi}\\ \lambda_{n_v\varpi}\end{bmatrix}\right\|=\left\|\begin{bmatrix}\dfrac{\vec{S}_{h\varpi}}{G}\\ \left(\dot{\mathbf{I}}'-\left|\dot{\mathbf{I}}'\right|\right)\times\vec{S}_{\varpi}\\ S_{\rho\varpi}\end{bmatrix}\right\},\end{gathered} \tag{3.38}$$

where $\vec{\lambda}_x=\left\{\lambda_{x,f}\right\}^T$, $\vec{\lambda}_y=\left\{\lambda_{y,f}\right\}^T$, $\vec{\lambda}_z=\left\{\lambda_{z,f}\right\}^T$, $\vec{\lambda}_{\varpi}=\left\{\lambda_{\varpi,f}\right\}^T$, $f=\overline{1,n_v-1}$ are the unknown column vectors of Lagrange multipliers consisting of n_v-1 elements;

$\lambda_{n_vx}, \lambda_{n_vy}, \lambda_{n_vz}, \lambda_{n_v\varpi}$ are the additional Lagrange multipliers.

The projection of the vector $\vec{b}_x=\left\{b_{x,j}\mid j=\overline{1,n_r}\right\}$ defined of the set of n_r unbranched sectional parts into the set of sectional segments $\vec{b}_x^{\varsigma}=\left\{b_{x,\kappa}^{\varsigma}\mid\kappa=\overline{1,n_{\varsigma}-1}\right\}$ can be written as: $b_{x,\kappa}^{\varsigma}=b_{x,j}\,\forall\kappa:\vec{s}_{\kappa}^{\varsigma}\subseteq\mathrm{R}_j^{\varsigma}$; and $b_{x,\kappa}^{\varsigma}=0\;\forall\kappa:\vec{s}_{\kappa}^{\varsigma}\bigcap\mathrm{R}_j^{\varsigma}=\varnothing$. Similarly, the column vectors $\vec{b}_y=\left\{b_{y,j}\mid j=\overline{1,n_r}\right\}$, $\vec{b}_z=\left\{b_{z,j}\mid j=\overline{1,n_r}\right\}$ and $\vec{b}_{\varpi}=\left\{b_{\varpi,j}\mid j=\overline{1,n_r}\right\}$ can be also projected into the set of sectional segments obtaining corresponded column vectors $\vec{b}_y^{\varsigma}=\left\{b_{y,\kappa}^{\varsigma}\mid\kappa=\overline{1,n_{\varsigma}-1}\right\}$, $\vec{b}_z^{\varsigma}=\left\{b_{z,\kappa}^{\varsigma}\mid\kappa=\overline{1,n_{\varsigma}-1}\right\}$ and $\vec{b}_{\varpi}^{\varsigma}=\left\{b_{\varpi,\kappa}^{\varsigma}\mid\kappa=\overline{1,n_{\varsigma}-1}\right\}$.

The following transformations for the first moments of inertia and for the sectorial moment of inertia should be performed, $\forall\kappa=\overline{1,n_{\varsigma}-1}$:

$$\overline{S}_{oz,\kappa}^{\varsigma}\leftarrow\left\{S_{oz,\kappa}^{\varsigma}-b_{z,\kappa}^{\varsigma}\right\};\ \overline{S}_{oy,\kappa}^{\varsigma}\leftarrow\left\{S_{oy,\kappa}^{\varsigma}-b_{y,\kappa}^{\varsigma}\right\} \tag{3.39}$$

$$\overline{S}_{o\varpi,\kappa}^{\varsigma}\leftarrow\left\{S_{o\varpi,\kappa}^{\varsigma}-b_{\varpi,\kappa}^{\varsigma}\right\};\ \tilde{S}_{o\varpi,\kappa}^{\varsigma}\leftarrow\left\{\overline{S}_{o\varpi,\kappa}^{\varsigma}-a_{\kappa}^{\varsigma}\frac{I_{\varpi}}{\Omega_0}\right\}. \tag{3.40}$$

Let us define the sets of shear forces flows values for the start, middle and end points at the middle line of the sectional segments $\mathbf{T}^{\varsigma,\text{st}}=\left\{T_{\kappa}^{\varsigma,\text{st}}\right\}$, $\mathbf{T}^{\varsigma,\text{mid}}=\left\{T_{\kappa}^{\varsigma,\text{mid}}\right\}$, $\mathbf{T}^{\varsigma,\text{end}}=\left\{T_{\kappa}^{\varsigma,\text{end}}\right\}$, $\kappa=\overline{1,n_{\varsigma}-1}$, consisting of $n_{\varsigma}-1$ elements (by the number of sectional segments) as presented below [22]:

$$T_{\kappa}^{\varsigma,\text{start}}=\frac{\wp H}{\Omega_0}a_{\kappa}^{\varsigma}-\frac{Q_y}{I_z}\overline{S}_{oz,\kappa}^{\varsigma,\text{start}}-\frac{Q_z}{I_y}\overline{S}_{oy,\kappa}^{\varsigma,\text{start}}-\frac{M_{\varpi}}{I_{\varpi}}\tilde{S}_{o\varpi,\kappa}^{\varsigma,\text{start}};\tag{3.41}$$

$$T_{\kappa}^{\varsigma,mid}=\frac{\wp H}{\Omega_0}a_{\kappa}^{\varsigma}-\frac{Q_y}{I_z}\overline{S}_{oz,\kappa}^{\varsigma,mid}-\frac{Q_z}{I_y}\overline{S}_{oy,\kappa}^{\varsigma,mid}-\frac{M_{\varpi}}{I_{\varpi}}\tilde{S}_{o\varpi,\kappa}^{\varsigma,mid};\tag{3.42}$$

$$T_{\kappa}^{\varsigma,end}=\frac{\wp H}{\Omega_0}a_{\kappa}^{\varsigma}-\frac{Q_y}{I_z}\overline{S}_{oz,\kappa}^{\varsigma,end}-\frac{Q_z}{I_y}\overline{S}_{oy,\kappa}^{\varsigma,end}-\frac{M_{\varpi}}{I_{\varpi}}\tilde{S}_{o\varpi,\kappa}^{\varsigma,end},\tag{3.43}$$

where the first moments of inertia $\overline{S}_{oz,\kappa}^{\varsigma}$, $\overline{S}_{oy,\kappa}^{\varsigma}$ and the sectorial moment of inertia $\tilde{S}_{o\varpi,\kappa}^{\varsigma}$ are calculated using transformations in Equations (3.39) and (3.40), respectively.

The shear stresses for each κ^{th} sectional segment $\tau^{\varsigma}=\left\{\vec{\tau}_{\kappa}^{\varsigma}=\left\{\tau_{\kappa}^{\varsigma,\text{start}},\tau_{\kappa}^{\varsigma,\text{mid}},\tau_{\kappa}^{\varsigma,\text{end}}\right\}\right\}$, $\kappa=\overline{1,n_{\varsigma}-1}$, can be calculated as presented below:

$$\tau_{\kappa}^{\varsigma}=\left\{\begin{array}{l}\tau_{\kappa}^{\varsigma,\text{start}}=\left|\frac{T_{\kappa}^{\varsigma,\text{start}}}{\delta_{\kappa}^{\varsigma}}\right|\pm\frac{(1-\wp)H\delta_{\kappa}^{\varsigma}}{I_k}\\ \tau_{\kappa}^{\varsigma,\text{mid}}=\left|\frac{T_{\kappa}^{\varsigma,\text{mid}}}{\delta_{\kappa}^{\varsigma}}\right|\pm\frac{(1-\wp)H\delta_{\kappa}^{\varsigma}}{I_k}\\ \tau_{\kappa}^{\varsigma,\text{end}}=\left|\frac{T_{\kappa}^{\varsigma,\text{end}}}{\delta_{\kappa}^{\varsigma}}\right|\pm\frac{(1-\wp)H\delta_{\kappa}^{\varsigma}}{I_k}\end{array}\right\},\tag{3.44}$$

where the torsion moment of inertia I_x and the parameter $\wp$ are calculated as:

$$I_x=I_k+I_{\Gamma}=\frac{1}{3}\sum_{\kappa=1}^{n_{\varsigma}-1}l_{\kappa}^{\varsigma}\left(\delta_{\kappa}^{\varsigma}\right)^3+I_{\Gamma};\tag{3.45}$$

$$\wp=1-\frac{I_k}{I_x}.\tag{3.46}$$

The components $\left|\frac{T_{\kappa}^{\varsigma,\text{start}}}{\delta_{\kappa}^{\varsigma}}\right|$, $\left|\frac{T_{\kappa}^{\varsigma,\text{mid}}}{\delta_{\kappa}^{\varsigma}}\right|$ and $\left|\frac{T_{\kappa}^{\varsigma,\text{end}}}{\delta_{\kappa}^{\varsigma}}\right|$ in Equation (3.44) define shear stresses values for the start, middle and end points at the middle line of κ^{th} sectional segment, accordingly. Besides, transition from the shear stresses related to the middle line of κ^{th} segment to the shear stresses at the outside longitudinal edges of this segment can be performed by addition or subtraction of the member $\frac{(1-\wp)}{I_k}H\delta_{\kappa}^{\varsigma}$.

3. Results and Discussion

3.1. Software implementation

The numerical algorithm developed and presented above has been implemented to the TONUS software (hereinafter – TONUS), which is a satellite of the SCAD Office environment [24], as shown in Figure 6. TONUS is intended to create cross-sections of thin-walled bars, to calculate their geometrical properties as well as to calculate normal, shear and equivalent stresses in these cross-sections [9]. TONUS allows to consider arbitrary (including open-closed) cross-sections of thin-walled bars. The cross-section of a thin-walled bar is constructed from the set of segments (stripes) by specifying node coordinates that define the position of segment ends as well as by specifying thicknesses for all segments.

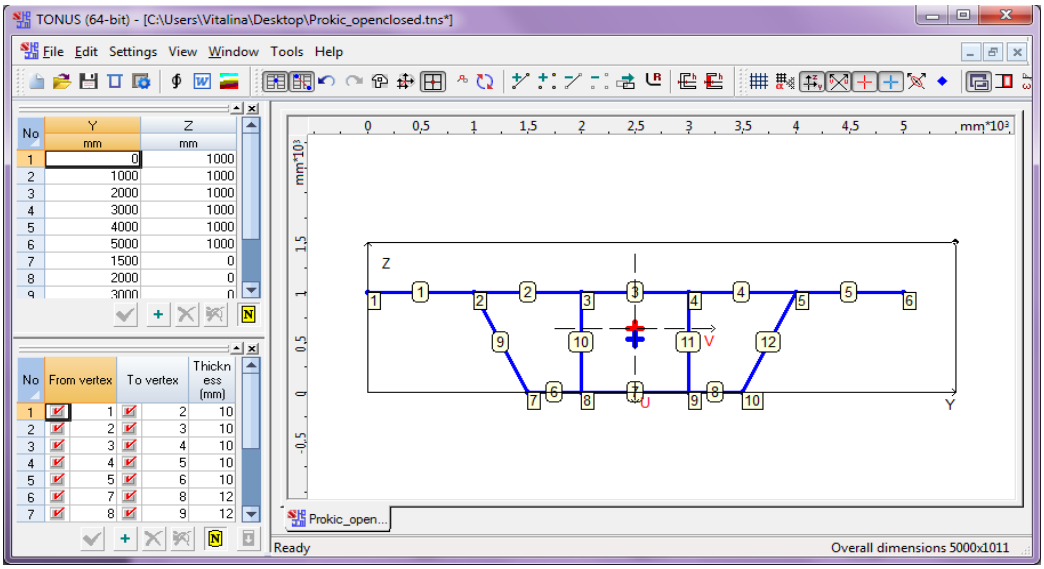

Figure 6. TONUS main window.

In addition to the calculation of geometrical properties for the cross-sections of thin-walled bars, TONUS also presents a sectorial coordinates diagram as well as static moment diagrams S_u, S_v and a first sectorial moment S_ω diagram.

To present normal, shear and equivalent stresses diagrams in the section of a thin-walled bar, the user should specify internal forces acting in the section. Initial data to construct normal stresses diagram include bending moments M_u and M_v relating to the main axis of inertia of the thin-walled bar cross-section, axial force N applied at the center of mass of the section, as well as warping bimoment B. Initial data to construct shear stresses diagram are shear forces Q_u and Q_v applied at the center of mass of the cross-section as well as total torque M_x and warping torque M_ω. In order to represent equivalent stresses diagram user should also specify a strength theory.

3.2. Example 1: open thin-walled cross-section

Let us consider an example of calculation of a thin-walled bar with open profile in order to validate the developed algorithm and verify the accuracy of the calculated sectorial cross-section properties and shear stresses caused by warping torsion.

Initial data for calculation are presented in Figure 7. The results of calculation, namely sectorial coordinates diagram ω [cm²], and shear stresses diagram related to the value of warping torque $\tau_\omega M_\omega^{-1} \times 10^7$ [cm⁻³], have been obtained in [18] and presented in Figure 8.

The results of calculation, namely sectorial coordinates ω, sectorial moment of inertia S_ω and shear stresses τ_ω caused by the warping torque M_ω = 10⁷ kN cm, have been also obtained using TONUS and presented in Figures 10–12.

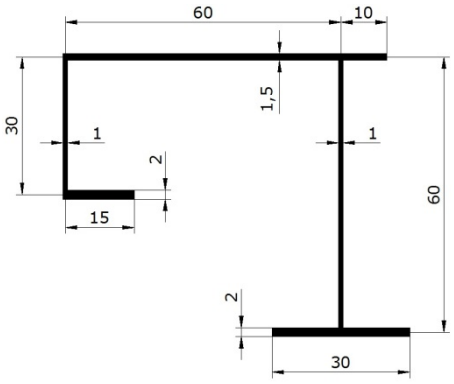

Figure 7. Dimensions [cm] of the open thin-walled section.

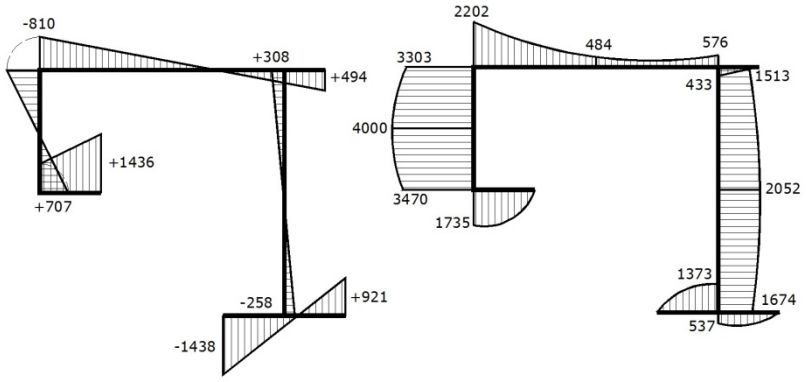

a *b*

Figure 8. Results of calculation according to [18]: *a* – sectorial coordinate ω [cm²]; *b* –shear stresses related to the warping torque $\tau_\omega M_\omega^{-1} \times 10^7$ [cm⁻³].

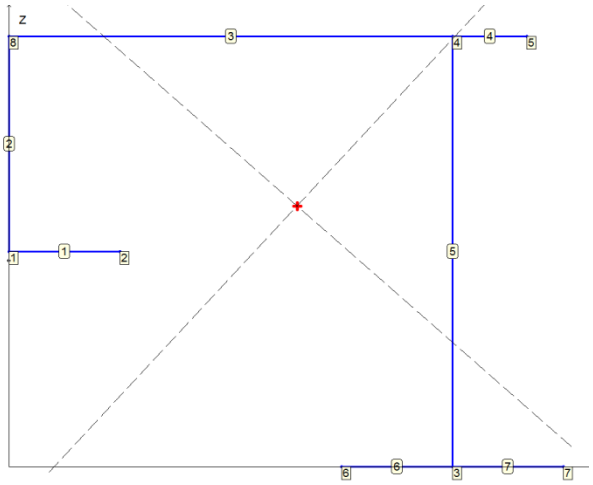

Figure 9. Considered cross-section with segments and points numbers.

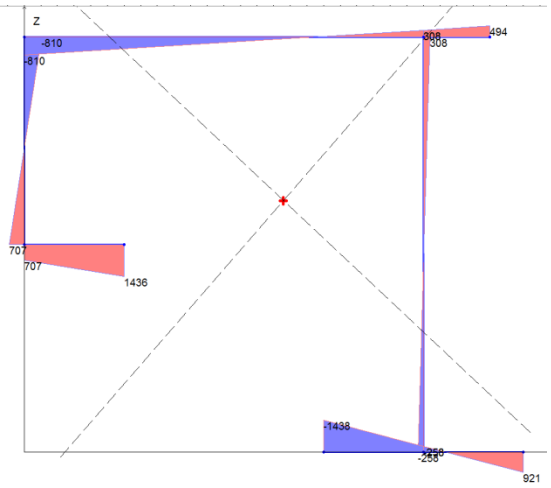

Figure 10. Results obtained using TONUS: sectorial coordinate ω [cm^2].

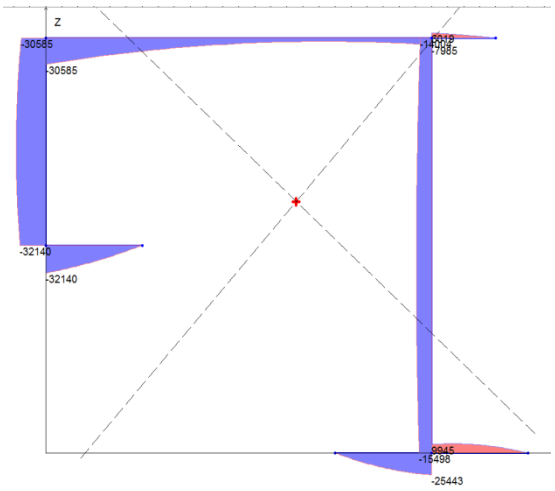

Figure 11. Results obtained using TONUS: sectorial moment of inertia S_ω [cm^4].

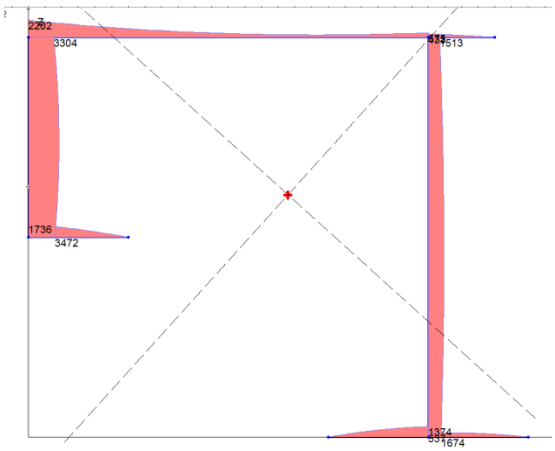

Figure 12. Results obtained using TONUS: modulus of shear stresses τ_ω [kN/cm^2] caused by warping torsion for the value of warping torque M_ω = 10^7 kN cm.

Table 1. Comparison of the first sectorial moment and shear stresses caused by the warping torque for the considered cross-section.

Section segment number (Figure 9)	Section point number (Figure 9)	First sectorial moment S_ω [cm^4]			Shear stresses τ_ω [kN/cm^2] (when M_ω = 10^7 kN cm)		
		[18]	TONUS	Deviation,%	[18]	TONUS	Deviation,%
1	1	32126	32140	0.04	1735	1736	0.06
1	2	0	0	0	0	0	0
2	1	32126	32140	0.04	3470	3472	0.06
2	8	30580	30585	0.02	3303	3304	0.06
3	8	30580	30585	0.02	2202	2202	0
3	4	7999	7985	0.18	576	575	0.17
4	4	6013	6019	0.1	433	432	0.23
4	5	0	0	0	0	0	0
5	4	14008	14004	0.03	1513	1513	0
5	3	15498	15498	0	1674	1674	0
6	6	0	0	0	0	0	0
6	3	25423	25443	0.08	1373	1374	0.07
7	3	9943	9945	0.02	537	537	0
7	7	0	0	0	0	0	0

Table 2. Comparison of sectorial coordinates for the considered cross-section.

Section point number (Figure 9)	Sectorial coordinate ω [cm^2]		
	[18]	TONUS	Deviation, %
1	707	707	0
2	1436	1436	0
3	–258	–258	0
4	308	308	0
5	494	494	0
6	–1438	–1438	0
7	921	921	0
8	–810	–810	0

Sectorial first moment of inertia and shear stresses caused by warping torsion, as well as sectorial coordinates for considered thin-walled bar cross-section are presented in Tables 1 and 2. The comparisons have been made with some results presented in [18], which represent exact results for the considered example. As it can be seen, the deviations do not exceed 0.25 % in all cases. It proves the validity of the results obtained using the developed software.

3.3. Example 2: open-closed multi-contour thin-walled cross-section

Let us consider an example of calculation of a thin-walled bar with open-closed multi-contour profile in order to validate developed algorithm and verify calculation accuracy for geometrical cross-section properties and shear stresses caused by warping torsion, as well as shear force. The initial data for calculation are presented in Figure 13.

The calculation results, namely sectorial coordinates diagram ϖ [cm^2], diagram of shear stresses caused by warping torsion related to the value of warping torque $\tau_{\varpi} M_{\varpi}^{-1} \times 10^7$ [cm^{-3}], as well as diagram of shear stresses caused by acting of shear force related to the value of shear force $\tau_u Q_u^{-1} \times 10^5$ [cm^{-2}] have been obtained by Prokić [18] and presented in Figure 14.

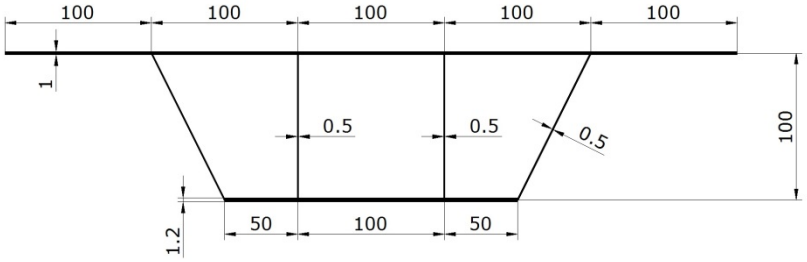

Figure 13. Dimensions [cm] of the open-closed multi-contour section of the thin-walled bar.

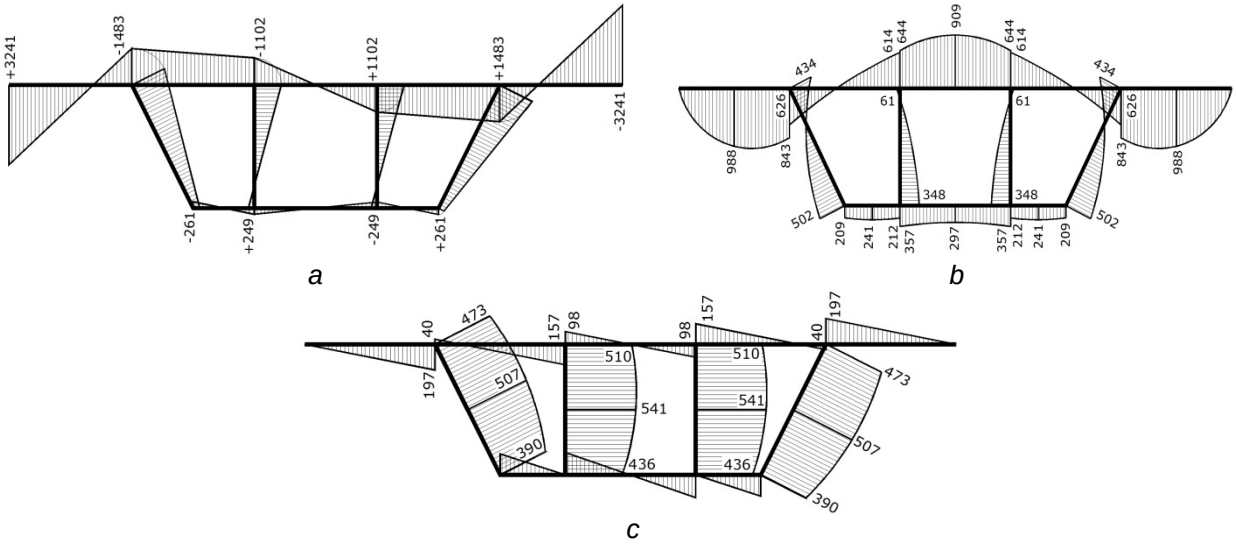

Figure 14. Results of calculations according to [18]: *a* – sectorial coordinates diagram ϖ [cm^2]; *b* – shear stresses diagram caused by warping torsion related to the value of the warping torque $\tau_{\varpi} M_{\varpi}^{-1} \times 10^7$ [cm^{-3}]; *c* – shear stresses diagram caused by shear force related to the value of shear force $\tau_u M_u^{-1} \times 10^5$ [cm^{-2}].

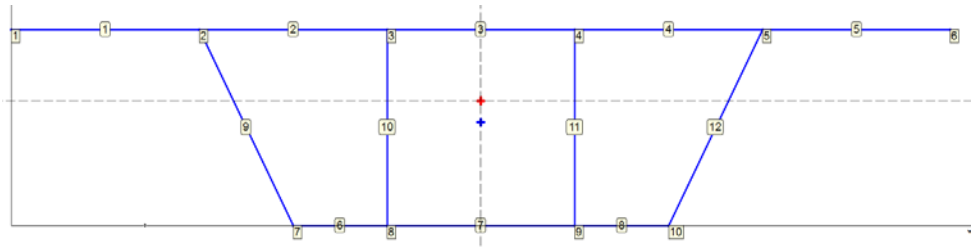

Figure 15. Cross-section with segments and points numbers.

The calculation results, namely sectorial coordinates ϖ, static moment S_v relating to the main axes of inertia $v - v$, first sectorial moment S_ϖ, shear stresses τ_u caused by shear force Q_u = 10^5 kN, as well as shear stresses τ_ϖ caused by warping torque M_ϖ = 10^7 kN cm for the considered cross-section section have been obtained using TONUS and presented in Figure 16.

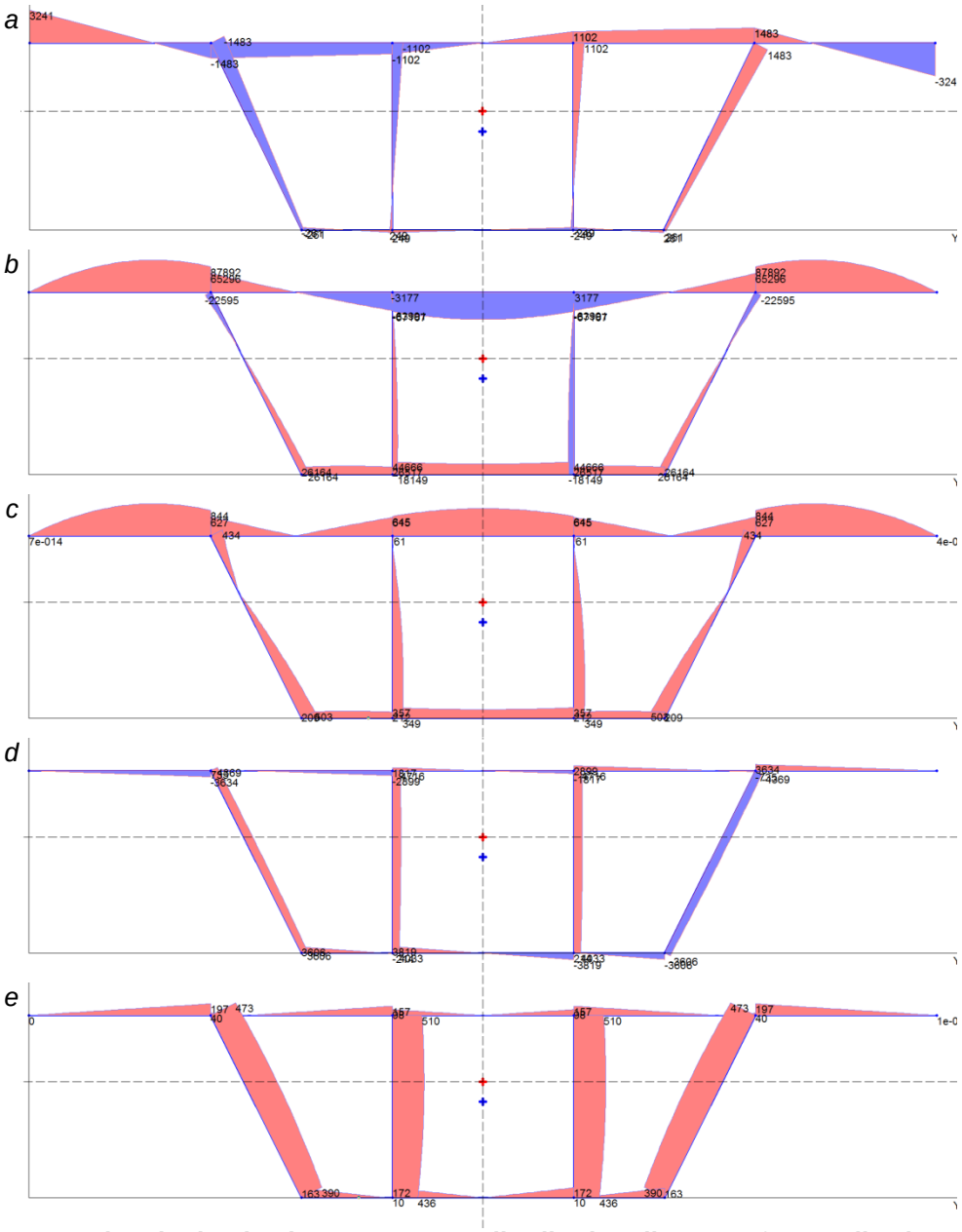

Figure 16. Results obtained using TONUS: *a* – distribution diagram of normalized sectorial coordinates ϖ [cm^2]; *b* – distribution diagram of first sectorial moment S_ϖ [cm^4]; *c* – distribution diagram of modulus of shear stresses τ_ϖ [kN/cm^2], constructed depending on the value of the warping torque M_ϖ = 10^7 kN cm; *d* – distribution diagram for the first moment S_v [cm^3] relating to the principle axis $v - v$; *e* – distribution diagram of modulus of shear stresses τ_u [kN/cm^2], constructed depending on the value of shear force Q_u = 10^5 kN.

First moment S_v and first sectorial moment S_ϖ, shear stresses τ_u and τ_ϖ caused by shear force Q_u and warping torque M_ϖ, respectively, as well as sectorial coordinates ϖ for the considered cross-section are presented in Tables 3–5. The comparisons have been made with some results presented in [18], which represent exact results for the considered example. The deviations are no more than 0.3 % in all design cases. It proves the validity of the results obtained using the developed software.

Table 3. Comparison of first moments for considered cross-section.

Section segment number (Figure 15)	Section point number (Figure 15)	First sectorial moment S_ϖ [cm^4]			First moment S_v [cm^3]		
		[18]	TONUS	Deviation,%	[18]	TONUS	Deviation,%
1	1	0	0	0	0	0	0
1	2	87776	87892	0.13	3643	3634	0.25
2	2	65181	65296	0.18	740	741	0.14
2	3	63932	64036	0.16	2903	2899	0.14
3	3	67055	67159	0.16	1812	1817	0.28
6	7	26114	26164	0.19	3595	3606	0.3
6	8	26489	26517	0.11	–	10	–
7	8	44606	44666	0.13	3816	3819	0.08
9	2	22595	22595	0	4373	4369	0.09
9	7	26135	26164	0.11	3606	3606	0
10	3	3176	3177	0.03	4715	4716	0.02
10	8	18117	18149	0.15	4031	4033	0.05

Table 4. Comparison of shear stresses caused by the warping torque, as well as by the shear force for the considered cross-section.

Section segment number (Figure 15)	Section point number (Figure 15)	Shear stresses τ_ϖ [kN/cm^2] (when M_ϖ = 10^7 kN cm)			Shear stresses τ_u [kN/cm^2] (when Q_u = 10^5 kN)		
		[18]	TONUS	Deviation, %	[18]	TONUS	Deviation, %
1	1	0	0	0	0	0	0
1	2	843	844	0.12	197	197	0
2	2	626	627	0.16	40	40	0
2	3	614	615	0.16	157	157	0
3	3	644	645	0.16	98	98	0
6	7	209	209	0	162	163	0.6
6	8	212	212	0	–	10	0
7	8	357	357	0	172	172	0
9	2	434	434	0	473	473	0
9	7	502	503	0.20	390	390	0
10	3	61	61	0	510	510	0
10	8	348	349	0.29	436	436	0

Table 5. Comparison of normalized sectorial coordinate for the considered cross-section.

Section point number (Figure 15)	Sectorial coordinate ϖ [cm^2]		
	[18]	TONUS	Deviation, %
1	+3241	+3241	0
2	–1483	–1483	0
3	–1102	–1102	0
7	–261	–261	0
8	+249	+249	0

4. Conclusions

The results of the presented study can be formulated as follow:

1. The searching problem of shear stresses outside longitudinal edges of an arbitrary cross-section (including open-closed multi-contour cross-sections) of a thin-walled bar subjected to the general load case has been considered in the paper.

2. The formulated problem has been transformed into a minimization problem of Castigliano's functional subject to constraints-equalities of shear forces flows equilibrium formulated for cross-section branch points as well as subject to an equilibrium equation for the whole cross-section relating to longitudinal axes of the thin-walled bar.

3. A detailed numerical algorithm intended to solve the searching problem of shear forces flows for an arbitrary cross-section of a thin-walled bar subjected to the general loading case using the mathematical apparatus of the graph theory has been developed. The algorithm is oriented on software implementation in systems of computer-aided design of the thin-walled structures.

4. The developed algorithm has been implemented to the TONUS software, which is a satellite of the SCAD Office environment.

5. Numerical examples for calculation of the thin-walled bars with open and open-closed multi-contour cross-sections have been considered in order to validate developed algorithm and verify calculation accuracy for sectorial cross-section geometrical properties and shear stresses caused by warping torque and shear forces.

6. Validity of the calculation results obtained using the developed software has been proven by considered examples.

References

1. Dowell, R.K., Johnson, T.P. Closed-form shear flow solution for box-girder bridges under torsion [Online]. Engineering Structures. 2012. No. 34. Pp. 383–390. URL: https://doi.org/10.1016/j.engstruct.2011.09.023
2. Shen, K., Wan, S., Mo, Y.L., Jiang, Z., Li, X. Behavior of single-box multi-cell box-girders with corrugated steel webs under pure torsion. Part II: Theoretical model and analysis [Online]. Thin-Walled Structures. 2018. No. 129. Pp. 558–572. URL: https://doi.org/10.1016/j.tws.2017.12.023
3. Shen, K., Wan, S., Mo, Y.L., Jiang, Z., Li, X.. Behavior of single-box multi-cell box-girders with corrugated steel webs under pure torsion. Part I: Experimental and numerical studies [Online]. Thin-Walled Structures. 2018. No. 129. Pp. 542–557. URL: https://doi.org/10.1016/j.tws.2017.10.038
4. Perelmuter, A.V., Slivker, V.I. Numerical structural analysis: models, methods and pitfalls. Springer-Verlag Berlin Heidelberg, 2003. 600 p.
5. Slivker, V.I. Mechanics of structural elements. Theory and applications. Springer-Verlag Berlin Heidelberg. 2007. 786 p.
6. Lalin, V., Rybakov, V., Sergey, A. The finite elements for design of frame of thin-walled beams. Applied Mechanics and materials. 2014. Vol. 578–579. Pp. 858–863. DOI: 10.4028/www.scientific.net/AMM.578-579.858
7. Lalin, V.V., Rybakov, V.A., Diakov, S.F., Kudinov, V.V., Orlova, E.S. The semi-shear theory of V.I. Slivker for the stability problems of thin-walled bars. Magazine of Civil Engineering. 2019. Vol. 87. Is. 3. Pp. 66–79.
8. Dyakov, S.F. Comparing the results of the thin-walled bar torsion problem according to Vlasov and Slivker theories [Online]. Structural mechanics of engineering constructions and buildings. 2013. No. 1. Pp. 24–31. URL: http://journals.rudn.ru/structural-mechanics/article/view/11128 (rus)
9. Yurchenko, V.V. Proyektirovaniye karkasov zdaniy iz tonkostennykh kholodnognutykh profiley v srede SCAD Office [Designing of steel frameworks from thin-walled cold-formed profiles in SCAD Office] [Online]. Magazine of Civil Engineering. 2010. No. 8. Pp. 38–46. URL: http://engstroy.spbstu.ru/index_2010_08/yurchenko_LSTK.pdf (rus)
10. Ádány, S., Schafer, B.W. Generalized constrained finite strip method for thin-walled members with arbitrary cross-section: Primary modes [Online]. Thin-Walled Structures. 2014. No. 84. Pp. 150–169. URL: https://doi.org/10.1016/j.tws.2014.06.001
11. Jönsson, J. Determiantion of shear stresses, warping functions and section properties of thin-walled beams using finite elements. Computer and Structures. 1998. No. 68. Pp. 393–410.
12. Sharafi, P., Teh, L.H., Hadi, M.N.S. Shape optimization of thin-walled steel sections using graph theory and ACO algorithm. Journal of Constructional Steel Research. 2014. No. 101. Pp. 331–341.
13. Tarjan, R. Depth-first search and linear graph algorithms. SIAM Journal Computing. 1972. No. 1. Pp. 146–60.
14. Alfano, G., Marotti de Sciarra, F., Rosati, L. Automatic analysis of multicell thin-walled sections. Computer and Structures. 1996. No. 59. Pp. 641–655.
15. Waldron, P. Sectorial properties of straight thin-walled beams. Computers and Structures. 1986. Vol. 24. Is. 1. Pp. 147–156.
16. Yoo, C.H. Cross-sectional properties of thin-walled multi-cellular section. Computer and Structures. 1986. No. 22. Pp. 53–61.
17. Yoo, C.H., Kang, J., Kim, K., Lee, K.C. Shear flow in thin-walled cellular sections [Online]. Thin-Walled Structures. 2011. 49(11). Pp. 1341–1347. URL: https://doi.org/10.1016/j.tws.2011.02.014
18. Prokić, A. Computer program for determination of geometrical properties of thin-walled beams with open-closed section. Computers and Structures. 2000. No. 74. Pp. 705–715.
19. Gurujee, C.S., Shah, K.R. A computer program for thin-walled frame analysis. Advances in Engineering Software. 1989. No. 11. Pp. 58–70.
20. Choudhary, G.K., Doshi, K.M. An algorithm for shear stress evaluation in ship hull girders [Online]. Ocean Engineering. 2015. 108(1). Pp. 678–691. URL: https://doi.org/10.1016/j.oceaneng.2015.08.048

21. Perelmuter, A., Yurchenko, V. Shear stresses in hybrid thin-walled section: development of detail numerical algorithm based on the graph theory. Proceedings of 3rd Polish Congress of Mechanics and 21st International Conference on Computer Methods in Mechanics. Short Papers. 2015. Vol. 2. Pp. 943–944.
22. Yurchenko, V. Searching shear forces flows for an arbitrary cross-section of a thin-walled bar: development of numerical algorithm based on the graph theory. International journal for computational civil and structural engineering. 2019. No. 15(1). Pp. 153–170.
23. San Francisco-Oakland Bay Bridge New East Span Skyway – San Francisco and Oakland, California. American Segmental Bridge Institute [Online]. URL: http://www.asbi-assoc.org/projects
24. URL: www.scadsoft.com

Contacts:

Vitalina Yurchenko, +38(063)8926491; vitalinay@rambler.ru

Инженерно-строительный журнал

ISSN 2071-0305

сайт журнала: http://engstroy.spbstu.ru/

DOI: 10.18720/MCE.92.1

Алгоритм определения потоков касательных усилий для произвольных сечений тонкостенных стержней

В. Юрченко*

Киевский национальный университет строительства и архитектуры, г. Киев, Украина

** E–mail: vitalinay@rambler.ru*

Ключевые слова: тонкостенный стержень, произвольное сечение, потоки касательных усилий, замкнутый контур, теория графов, численный алгоритм, численные примеры, программная реализация

Аннотация. Разработка универсального программного комплекса для расчета и проектирования тонкостенных стержневых элементов конструкций остается актуальной задачей. Несмотря на превалирующее влияние нормальных напряжений на напряженно-деформированное состояние тонкостенных стержней, проверка несущей способности таких элементов должна выполняться, принимая во внимание также и значения касательных напряжений. В связи с этим рассмотрена задача поиска значений потоков касательных усилий для произвольного сечения (открыто-замкнутого многоконтурного сечения) тонкостенного стержня для общего случая нагружения. Сформулированная задача приведена к задаче математического программирования, а именно к задаче поиска значений неизвестных потоков касательных напряжений, обеспечивающих наименьшее значение функционала Кастильяно при удовлетворении ограничений равновесия потоков в точках ветвления сечения, а также при удовлетворении уравнения равновесия всего сечения тонкостенного стержня относительно продольной оси. Разработан детальный алгоритм численного решения сформулированной задачи с использованием математического аппарата теории графов, ориентированный на программную реализацию в системах автоматизированного проектирования тонкостенных стержневых систем. Выполнена программная реализация разработанного алгоритма в среде вычислительного комплекса SCAD Office в программе ТОНУС. С целью верификации разработанного алгоритма и проверки точности вычислений геометрических характеристик и касательных напряжений рассмотрены примеры расчета тонкостенных стержневых элементов открытого и открыто-замкнутого многоконтурного сечений. На рассмотренных примерах доказана достоверность результатов, получаемых при использовании разработанного программного обеспечения.

Литература

1. Dowell R.K., Johnson T.P. Closed-form shear flow solution for box–girder bridges under torsion [Электронный ресурс] // Engineering Structures. 2012. No. 34. Pp. 383–390. URL: https://doi.org/10.1016/j.engstruct.2011.09.023
2. Shen K., Wan S., Mo Y.L., Jiang Z., Li X. Behavior of single-box multi-cell box-girders with corrugated steel webs under pure torsion. Part II: Theoretical model and analysis [Электронный ресурс] // Thin-Walled Structures. 2018. No. 129. Pp. 558–572. URL: https://doi.org/10.1016/j.tws.2017.12.023
3. Shen K., Wan S., Mo Y.L., Jiang Z., Li X. Behavior of single-box multi-cell box-girders with corrugated steel webs under pure torsion. Part I: Experimental and numerical studies [Электронный ресурс] // Thin-Walled Structures. 2018. No. 129. Pp. 542–557. URL: https://doi.org/10.1016/j.tws.2017.10.038
4. Perelmuter A.V., Slivker V.I. Numerical structural analysis: models, methods and pitfalls. Springer-Verlag Berlin Heidelberg, 2003. 600 p.
5. Slivker V.I. Mechanics of structural elements. Theory and applications. Springer-Verlag Berlin Heidelberg, 2007. 786 p.
6. Lalin V., Rybakov V., Sergey A. The finite elements for design of frame of thin-walled beams [Электронный ресурс] // Applied Mechanics and materials. 2014. Vol. 578–579. Pp. 858–863. URL: 10.4028/www.scientific.net/AMM.578-579.858
7. Лалин В.В., Рыбаков В.А., Дьяков С.Ф., Кудинов В.В., Орлова Е.С. Полусдвиговая теория В.И. Сливкера в задачах устойчивости тонкостенных стержней // Инженерно-строительный журнал. 2019. № 3(87). С. 66–79. DOI: 10.18720/MCE.87.6
8. Дьяков С.Ф. Сравнительный анализ задачи кручения тонкостенного стержня по моделям Власова и Сливкера [Электронный ресурс] // Строительная механика инженерных конструкций и сооружений. Обзорно-аналитический и научно-технический журнал. 2013. № 1. С. 24–31. URL: http://journals.rudn.ru/structural-mechanics/article/view/11128
9. Юрченко В.В. Проектирование каркасов зданий из тонкостенных холодногнутых профилей в среде SCAD Office // Инженерно-строительный журнал. 2010. № 8(18). С. 38-4. DOI: 10.18720/MCE.18.7.
10. Ádány S., Schafer B.W. Generalized constrained finite strip method for thin-walled members with arbitrary cross-section: Primary modes [Электронный ресурс] // Thin-Walled Structures. 2014. No. 84. Pp. 150–169. URL: https://doi.org/10.1016/j.tws.2014.06.001

11. Jönsson J. Determiantion of shear stresses, warping functions and section properties of thin-walled beams using finite elements // Computer and Structures. 1998. No. 68. Pp. 393–410.
12. Sharafi P., Teh L.H., Hadi M.N.S. Shape optimization of thin-walled steel sections using graph theory and ACO algorithm // Journal of Constructional Steel Research. 2014. No. 101. Pp. 331–341.
13. Tarjan R. Depth-first search and linear graph algorithms // SIAM Journal Computing. 1972. Np. 1. Pp. 146–60.
14. Alfano G., Marotti de Sciarra F., Rosati L. Automatic analysis of multicell thin-walled sections // Computer and Structures. 1996. No. 59. Pp. 641–55.
15. Waldron P. Sectorial properties of straight thin-walled beams // Computers and Structures. 1986. Vol. 24. Is. 1. Pp. 147–156.
16. Yoo C.H. Cross-sectional properties of thin-walled multi-cellular section // Computer and Structures. 1986. No. 22. Pp. 53–61.
17. Yoo C.H., Kang J., Kim K., Lee K.C. Shear flow in thin-walled cellular sections [Электронный ресурс] // Thin-Walled Structures. 2011. No. 49(11). Pp. 1341–1347. URL: https://doi.org/10.1016/j.tws.2011.02.014
18. Prokić A. Computer program for determination of geometrical properties of thin-walled beams with open-closed section // Computers and Structures. 2000. No. 74. Pp. 705–715.
19. Gurujee C.S., Shah K.R. A computer program for thin-walled frame analysis // Advances in Engineering Software. 1989. No. 11. Pp. 58–70.
20. Choudhary G.K., Doshi K.M. An algorithm for shear stress evaluation in ship hull girders [Электронный ресурс] // Ocean Engineering. 2015. No. 108(1). Pp. 678–691. URL: https://doi.org/10.1016/j.oceaneng.2015.08.048
21. Perelmuter A., Yurchenko V. Shear stresses in hybrid thin-walled section: development of detail numerical algorithm based on the graph theory // Proceedings of 3rd Polish Congress of Mechanics and 21st International Conference on Computer Methods in Mechanics. Short Papers. 2015. Vol. 2. Pp. 943–944.
22. Yurchenko V. Searching shear forces flows for an arbitrary cross-section of a thin-walled bar: development of numerical algorithm based on the graph theory // International journal for computational civil and structural engineering. 2019. No. 15(1). Pp. 153–170.
23. San Francisco-Oakland Bay Bridge New East Span Skyway – San Francisco and Oakland, California [Электронный ресурс]. American Segmental Bridge Institute. URL: http://www.asbi-assoc.org/projects.
24. URL: www.scadsoft.com

Контактные данные:

Виталина Юрченко, +38(063)8926491; Эл. почта: vitalinay@rambler.ru